

Universal mechanism of (semi-classical) deconfinement and θ -dependence for all simple groups

Erich Poppitz,^{1,*} Thomas Schäfer,^{2,†} Mithat Ünsal^{3,‡}

¹*Department of Physics, University of Toronto, Toronto, ON M5S 1A7, Canada*

²*Department of Physics, North Carolina State University, Raleigh, NC 27695, USA*

³*Department of Physics and Astronomy, SFSU, San Francisco, CA 94132, USA*

ABSTRACT: Using the twisted partition function on $\mathbb{R}^3 \times \mathbb{S}^1$, we argue that the deconfinement phase transition in pure Yang-Mills theory for all simple gauge groups is continuously connected to a quantum phase transition that can be studied in a controlled way. We explicitly consider two classes of theories, gauge theories with a center symmetry, such as $SU(N_c)$ gauge theory for arbitrary N_c , and theories without a center symmetry, such as G_2 gauge theory. The mechanism governing the phase transition is universal and valid for all simple groups. The perturbative one-loop potential as well as monopole-instantons generate attraction among the eigenvalues of the Wilson line. This is counter-acted by neutral bions — topological excitations which generate eigenvalue repulsion for all simple groups. The transition is driven by the competition between these three effects. We study the transition in more detail for the gauge groups $SU(N_c)$, $N_c \geq 3$, and G_2 . In the case of G_2 there is no change of symmetry, but the expectation value of the Wilson line exhibits a discontinuity. We also examine the effect of the θ -angle on the phase transition and critical temperature $T_c(\theta)$. The critical temperature is a multi-branched function, which has a minimum at $\theta = \pi$ as a result of topological interference.

*poppitz@physics.utoronto.ca

†tmschaef@ncsu.edu

‡unsal@sfsu.edu

Contents

1. Introduction	1
1.1 Twisted partition function and continuity of the deconfinement transition between weak and strong coupling	2
1.2 Review of the dynamics for $\mathbf{m} = \mathbf{0}$ and small- \mathbf{L}	4
1.3 Phase transition in the small $\mathbf{m}\text{-}\mathbf{L}$ regime and universal aspects	5
2. $SU(N_c)$, $N_c \geq 3$: First order center symmetry changing phase transition	6
2.1 Relevant scales and two large- N_c limits: 't Hooft vs. Abelian	7
2.2 The bion and monopole potentials in softly-broken $SU(N_c)$ theory on $\mathbb{R}^3 \times \mathbb{S}^1$	9
2.3 The perturbative potential for arbitrary N_c	11
2.4 The phase transition and the limits of metastability for $N_c \geq 3$	12
2.5 More on the (abelian) large- N_c limit and (evading) the Hagedorn instability	15
3. θ-dependence of the phase transition and topological interference	17
3.1 θ -dependence of \mathbf{c}_m^{cr} for $N_c = 2$	19
4. G_2: First order transition without symmetry breaking	20
5. Weak vs. strong coupling non-trivial Wilson line holonomy	24
5.1 What changes between the semi-classical and strongly coupled deconfinement transitions?	25
6. Prospects	26

1. Introduction

In our recent work, we studied a semi-classical mechanism for the center symmetry changing phase transition in four dimensional non-abelian $SU(2)$ gauge theory [1]. The main idea of that work was to use continuity and the notion of a twisted partition function. We argued that the deconfining phase transition of pure Yang-Mills theory on $\mathbb{R}^3 \times \mathbb{S}_\beta^1$, which takes place at strong coupling, is continuously connected to a quantum phase transition that can be studied reliably, albeit using non-perturbative methods, at weak coupling.

The most important non-perturbative effect that arises in the weak coupling realization of the center symmetry changing phase transition is governed by a new class of topological objects, called “neutral bions”. These objects are related to four dimensional instantons, but their physical effects are quite different. The 't Hooft vertex for a neutral bion induces a

\mathfrak{g}	G	$G_{\text{ad}} := G/Z(G)$	$\pi_1(G_{\text{ad}}) = Z(G)$
A_{N-1}	$SU(N)$	$PSU(N)$	\mathbb{Z}_N
B_N	$Spin(2N+1)$	$SO(2N+1)$	\mathbb{Z}_2
C_N	$Sp(N)$ or $USp(2N)$	$PSp(N)$	\mathbb{Z}_2
D_{2N}	$Spin(4N)$	$PSO(4N)$	$\mathbb{Z}_2 \times \mathbb{Z}_2$
D_{2N+1}	$Spin(4N+2)$	$PSO(4N+2)$	\mathbb{Z}_4
E_6	E_6	E_6^{-78}	\mathbb{Z}_3
E_7	E_7	E_7^{-133}	\mathbb{Z}_2
E_8	E_8	E_8	1
F_4	F_4	F_4	1
G_2	G_2	G_2	1

Table 1: The simple Lie algebras \mathfrak{g} together with their associated compact simply-connected Lie groups G and the compact adjoint Lie groups G_{ad} . The last column lists the center symmetry of G , which is isomorphic to the fundamental group of G_{ad} .

center-stabilizing potential in $SU(2)$ theory, by generating a repulsion among the eigenvalues of the Wilson line.¹ This effect counter-acts the center-destabilizing perturbative potential for the Wilson line, which leads to an attraction among the eigenvalues [3]. In our previous work we showed that the monopole-instanton amplitudes also lead to an attraction among the eigenvalues of Wilson line. We systematically studied the competition between these three effects in the case of $SU(2)$ gauge theory. We observed that the twisted partition function on $\mathbb{R}^3 \times \mathbb{S}^1$ exhibits a second order phase transition, consistent with the second order transition observed in lattice gauge simulations of thermal $SU(2)$ Yang Mills theory.

In the present work, our goal is two-fold:

- a) to generalize the phase transition mechanism in $SU(2)$ to arbitrary compact simply-connected Lie groups, G , including the theories without a center, G_2, F_4, E_8 .
- b) to understand the topological θ -angle dependence of the critical temperature T_c .

For convenience, we list the simple Lie algebras \mathfrak{g} together with their associated compact simply-connected Lie groups G and the compact adjoint Lie groups G_{ad} in Table 1. The last column lists the center group of G , which is isomorphic to the fundamental group of G_{ad} . For theories with adjoint matter, the center symmetry is the same as the center group.

1.1 Twisted partition function and continuity of the deconfinement transition between weak and strong coupling

We consider Yang-Mills (YM) theory with one adjoint Weyl fermion with mass m . In the chiral limit this theory reduces to $\mathcal{N} = 1$ supersymmetric YM theory, and in the limit $m \rightarrow \infty$

¹For this reason, we sometimes refer to the neutral bion in theories with a center symmetry as “center-stabilizing bion” [2].

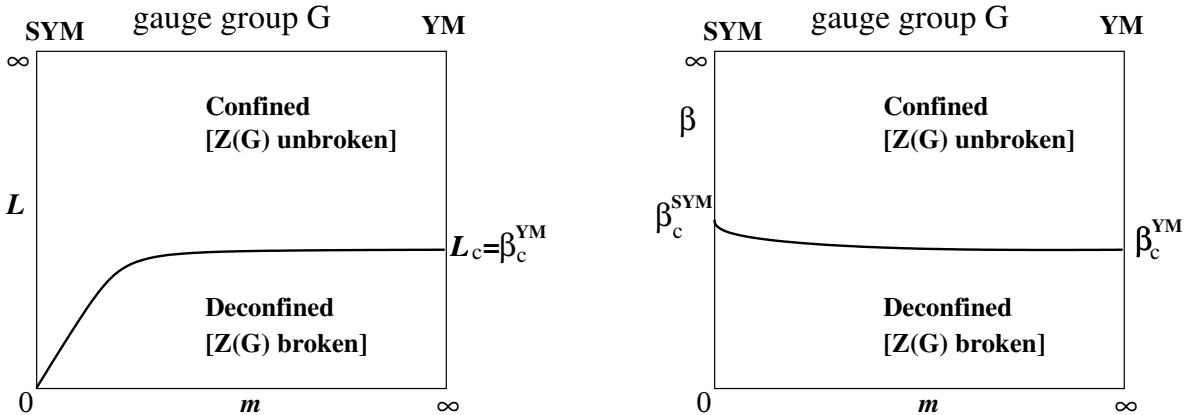


Figure 1: Phase diagram of Yang Mills (YM) theory with an arbitrary simply-connected gauge group G and a single Weyl fermion of mass m in the adjoint representation, subject to periodic (left) and anti-periodic (right) boundary conditions on $\mathbb{R}^3 \times S^1$. **Right:** For the ordinary partition function the transition occurs at a critical temperature of order Λ , and is not accessible by analytical means. **Left:** In the case of the twisted partition function, the thermal deconfinement phase transition in pure Yang Mills theory, corresponding to the limit $m \rightarrow \infty$, is conjectured to be continuously connected to a quantum phase transition in supersymmetric Yang Mills (SYM) theory deformed by a gluino mass term. For small m , the transition takes place as small L and is analytically tractable. For theories without center symmetry, there is no symmetry breaking associated with the transition.

it corresponds to pure YM theory. Let H and F denote the Hamiltonian and fermion number operator, respectively, and L the circumference of the S^1 circle. We introduce the twisted (non-thermal) partition function:

$$\tilde{Z}(L, m) = \text{tr} [e^{-LH} (-1)^F] = \text{tr} [e^{-LH + i\pi F}] , \quad (1.1)$$

which, when viewed as a function of fermion mass, interpolates between the supersymmetric (Witten) index and the ordinary thermal partition function of the pure Yang-Mills theory. Namely,

$$\begin{aligned} \tilde{Z}(L, m = 0) &= I_S(G), \\ \tilde{Z}(L, m = \infty) &= Z^{\text{YM}}(\beta), \quad L \equiv \beta , \end{aligned} \quad (1.2)$$

where $I_S(G) = h^\vee$ is the index, which is equal to an invariant h^\vee (independent of L) associated with the group G and called the dual Coxeter number (h^\vee equals N_c for $SU(N_c)$). Since $d\tilde{Z}(L, 0)/dL = 0$ for any L , there is no phase transition at $m = 0$ [4–6]. $Z^{\text{YM}}(\beta)$ is the partition function of the pure Yang-Mills theory. Eqs. (1.1) and (1.2) permit us to continue the deconfinement phase transition in pure YM theory to a semi-classically calculable transition in the small L - m regime as shown in Fig. 1.

1.2 Review of the dynamics for $\mathfrak{m} = 0$ and small- L

The dynamics of $\mathcal{N} = 1$ SYM theory with gauge group G in the small- L weak coupling regime is that of the abelianized theory, $U(1)^r$, where $r = \text{rank}(\mathfrak{g})$ is the rank of the Lie algebra of G [4–6]. The abelian description is valid at distance scales $\gtrsim Lr/2\pi$ [7]. This follows from the fact that the Wilson line holonomy behaves as a compact “adjoint Higgs field” in the weak coupling regime. We note that there is no such description at strong coupling, see the detailed discussion in Section 5. In a Euclidean context, the long distance theory is described as a dilute gas of topological 1-defects (item (i) below) and 2-defects (items (ii) and (iii)):

- (i) monopole-instantons \mathcal{M}_i with $i = 1, \dots, \text{rank}(\mathfrak{g}) + 1$,
- (ii) magnetic bions $\mathcal{B}_{ij} = [\mathcal{M}_i \overline{\mathcal{M}}_j]$, $\forall \hat{A}_{ij} < 0$,
- (iii) neutral bions $\mathcal{B}_{ii} = [\mathcal{M}_i \overline{\mathcal{M}}_i]$, $\forall \hat{A}_{ii} > 0$.

Here, \hat{A}_{ij} is the extended Cartan matrix of G . Small 4d instantons are responsible for breaking the anomalous axial $U(1)_A$ symmetry down to an anomaly free discrete subgroup, \mathbb{Z}_{2h^\vee} . But apart from that, they have no sizable impact to any physical phenomena in this regime. In the small- L regime, 4d instantons can be viewed as composites of the monopole-instantons, i.e., $\mathcal{I}_{4d} \sim \prod_{j=0}^r [\mathcal{M}_j]^{k_j^\vee}$, where k_j^\vee are dual Kac-labels (or co-marks; equal to unity for $SU(N_c)$) and $\sum_{j=0}^r k_j^\vee = h^\vee = I_S(G)$ is the dual Coxeter number. This formula embodies the physics of fractionalization of a large 4d instanton $\gtrsim Lr$ into k_j^\vee monopole-instantons of type \mathcal{M}_j , each of which carry two adjoint fermionic zero-modes.²

Since large 4d-instantons do not exist in this regime the problem of the breakdown of the dilute instanton gas approximation, which follows from the fact that instanton size is a modulus, is avoided. Moreover, since the 1-defects and 2-defects obey a separation of scales,

$$r_m \ll r_b \ll d_{m-m} \ll d_{b-b}, \quad (1.3)$$

the treatment of monopole-instantons (\mathcal{M}_i) and topological molecules (\mathcal{B}_{ij}) in the dilute-gas approximation and the effective theory derived from their proliferation in the vacuum is reliable. This is depicted in Fig. 2: r_m and r_b are the typical sizes of a monopole-instanton and bion events, and d_{m-m} and d_{b-b} are the typical inter-monopole-instanton and inter-bion separation. For a detailed discussion of the scales, see [14].

Monopole-instantons have two fermionic zero modes associated with a vertex of the form $\frac{\partial^2 W}{\partial \Phi_i \partial \Phi_j} \psi_i \psi_j \leftrightarrow \sum_k \mathcal{M}_k$, where $W(\Phi_i)$ is the superpotential of the effective theory. This means that the superpotential can be extracted from the monopole amplitude, but it does not imply that the mass gap for bosonic fluctuations is generated by monopoles, as is evident from the existence of a fermionic bilinear in the amplitude. The bosonic potential can be computed from the superpotential, $V = \sum_i |\frac{\partial W}{\partial \Phi_i}|^2 \leftrightarrow \sum_{i,j} \mathcal{B}_{ij}$, but the physical mechanism

²The topological classification of finite action solutions on $\mathbb{R}^3 \times \mathbb{S}^1$ can be found in [3]. Monopole constituents of the instanton (caloron) solution for non-trivial holonomy were found in [8,9], and the relevant index theorem is discussed in [10,11]. The monopole vertex for general gauge group can be found in [6]. Magnetic bions are studied in [12,13], and neutral bions are discussed in [1,2,14].

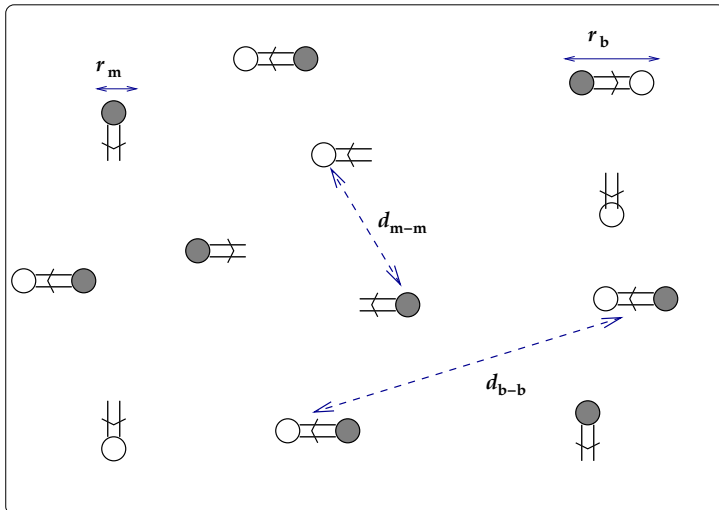


Figure 2: The Euclidean vacuum of the small- m , L theory can be described as a plasma of monopole-instantons (gray circles) and anti-monopole-instantons (white circles) with fermionic zero modes (unpaired arrows). The paired events are magnetic and neutral bions. Neutral bion amplitudes generate repulsion among the eigenvalues of the Wilson line and magnetic bions generate a mass gap for gauge fluctuations via a generalization of the Polyakov mechanism to a locally 4d theory.

which generates the bosonic potential and the mass gap for bosonic fluctuations is due to bions, correlated monopole-anti-monopole instantons without any fermionic zero modes. The bosonic potential also has h^\vee minima, leading, at weak coupling, to the spontaneous breaking of the discrete chiral symmetry, $\mathbb{Z}_{2h^\vee} \rightarrow \mathbb{Z}_2$. This, in turn, generates a dynamical mass for fermions. The importance of this point of view, apart from providing the correct interpretation of the physical phenomena governing the dynamics in the supersymmetric theory, is that semi-classical monopole and bion amplitudes also exist in non-supersymmetric theories, where the bosonic potential cannot be extracted from the super-potential [2, 12–14].

1.3 Phase transition in the small m - L regime and universal aspects

There are two main effects of adding a small fermion mass term. The mass term lifts the zero modes of the monopole-instantons. This implies that there is a non-zero monopole-instanton contribution to the bosonic potential. The mass term also breaks supersymmetry, which leads to a perturbative contribution to the potential for the holonomy [3]. Studying the competition between these effects and the bion induced potential already present at $m = 0$ shows that there is a phase transition at some critical compactification scale that grows with m . We find a description of this phase transition valid for *all* Lie groups, G :

1. Neutral bions *always* generate repulsion among the eigenvalues of the Wilson line around S^1 . For theories with a \mathbb{Z}_N center symmetry, the repulsion leads to a \mathbb{Z}_N -symmetric distribution, while for theories without a center symmetry, it leads to a non-degenerate distribution of eigenvalues, as we show explicitly for G_2 .

2. Monopole-instantons, along with the perturbative potential for the Wilson line, lead to an attractive interaction between the eigenvalues of the Wilson line. This interaction increases with m . Monopoles prefer configurations in which the eigenvalues accumulate. This leads to center-instability whenever $Z(G)$ is non-trivial and to eigenvalue bunching whenever $Z(G)$ is trivial.
3. Magnetic bions lead to an attraction among the eigenvalues of the Wilson line. They also generate a mass gap for gauge fluctuations, and they are responsible for the confinement of electric charges. However, the combined effect of neutral and magnetic bions (which are of the same order in the semi-classical expansion) always generates a repulsion among eigenvalues.
4. The competition of neutral and magnetic bions on the one hand and monopole-instanton and perturbative effects on the other hand is responsible for the semi-classical realization of deconfinement. For all gauge groups but G_2, F_4, E_8 , this phase transition is associated with a change in the center symmetry realization. For $SU(N_c)$ with $N_c \geq 3$, we find a first order phase transition associated with a change in the center symmetry realization. In earlier work, we found a second order phase transition for $N_c = 2$ [1]. In theories without a center symmetry, we find a first order transition accompanied by a jump in the Polyakov loop. These findings agree with lattice results (see [15–17], as well as [18] for a recent review), providing support for the conjectured continuity of the deconfinement transition depicted in Fig. 1.

Finally, we investigate the topological θ -angle dependence of the twisted partition function. As is well-known, turning on a θ -angle introduces a sign problem in the Euclidean path integral formulation. The semi-classical manifestation of the sign problem is a complex fugacity of monopole-instantons. The phase of the amplitude generates interference between Euclidean path histories, which can be interpreted as the analytic continuation of Aharonov-Bohm type interference. We refer to this phenomenon as “topological interference”. In the case of finite rank gauge groups topological interference leads to θ dependence of the critical temperature. The minimum T_c occurs at $\theta = \pi$. At this point the θ dependence is non-analytic, and all theories have two degenerate vacua in the confined phase. At $N = \infty$ the critical temperature is independent of θ .

2. $SU(N_c)$, $N_c \geq 3$: First order center symmetry changing phase transition

As reviewed in Section 1.2, at sufficiently small L the supersymmetric $SU(N_c)$ theory on $\mathbb{R}^3 \times \mathbb{S}^1$ dynamically abelianizes down to $U(1)^{N_c-1}$ at distances larger than $LN_c/2\pi$. In this regime the light bosonic fields are the $N_c - 1$ dual photon fields $\vec{\sigma}$ (a $N_c - 1$ -dimensional vector) and their scalar superpartners $\vec{\phi}$, which are the “uneaten” components of the gauge

connection along \mathbb{S}^1 . It is convenient to expand the fields $\vec{\phi}$ and $\vec{\sigma}$ as follows:

$$\begin{aligned}\vec{\phi} &\equiv \frac{2\pi}{N_c} \vec{\rho} + \frac{g^2}{4\pi} \vec{b}', \\ \vec{\sigma} + \frac{\theta \vec{\phi}}{2\pi} &\equiv \frac{2\pi k + \theta}{N_c} \vec{\rho} + \vec{\sigma}' .\end{aligned}\tag{2.1}$$

The primed fields describe the fluctuations of the fields $\vec{\phi}$ and $\vec{\sigma}$ around their supersymmetric and center-symmetric ground state. For every N_c the supersymmetric ground state is labeled by an integer $k = 1, \dots, N_c$, the vacuum angle θ , and the Weyl vector $\vec{\rho}$. The integer k corresponds to a choice of vacuum corresponding to the spontaneous breaking of the anomaly-free discrete chiral (R -) symmetry, $\mathbb{Z}_{2N_c} \rightarrow \mathbb{Z}_2$.

We normalize the $SU(N_c)$ Cartan generators $\vec{H} = (H_1, \dots, H_{N_c-1})$ by $\text{tr}[H_a H_b] = \delta_{ab}$. All the $SU(N_c)$ roots have length squared equal to 2, and the roots and co-roots, $\vec{\alpha}$ and $\vec{\alpha}^*$, as well as the fundamental weights and co-weights, $\vec{\omega}$ and $\vec{\omega}^*$, are the same. The Weyl vector is given by $\vec{\rho} = \sum_i \vec{\omega}_i$. The fundamental weights obey $\vec{\omega}_i \cdot \vec{\alpha}_j = \delta_{ij}$ ($i, j = 1, \dots, N_c - 1$), and the Weyl vector obeys $\vec{\rho} \cdot \vec{\alpha}_i = 1$, for $i = 1, \dots, N_c - 1$, and $\vec{\rho} \cdot \vec{\alpha}_{N_c} = 1 - N_c$.

The fields \vec{b}' and $\vec{\sigma}'$ in (2.1) are periodic,

$$\vec{b}' \sim \vec{b}' + \frac{8\pi^2}{g^2} \vec{\omega}, \quad \vec{\sigma}' \sim \vec{\sigma}' + 2\pi \vec{\omega} .\tag{2.2}$$

Note that for small g periodicity of \vec{b}' is irrelevant. The gauge holonomy (Wilson loop around \mathbb{S}_L^1) in terms of the fields (2.1) is given by:

$$\Omega = \exp \left(i \frac{2\pi}{N_c} \vec{H} \cdot \vec{\rho} + i \frac{g^2}{4\pi} \vec{H} \cdot \vec{b}' \right) .\tag{2.3}$$

At $\vec{b}' = 0$, Ω obeys $\text{tr} \Omega^n = 0, \forall n \neq 0 \pmod{N_c}$. We note that $\text{tr} \Omega^n$ are order parameters of the \mathbb{Z}_{N_c} global center symmetry that the adjoint-fermion $SU(N_c)$ theory acquires when compactified on $\mathbb{R}^3 \times \mathbb{S}_L^1$ and that center symmetry is unbroken in any of the N_c supersymmetric vacua.

It is also important to note that the Wilson line that satisfies $\langle \text{tr} \Omega^n \rangle = 0$ at weak coupling is associated with the eigenvalue configuration depicted on Figure 3(b). We refer to this type of gauge holonomy as weak coupling non-trivial holonomy. At strong coupling, there is no adjoint Higgsing, as the fluctuations of the eigenvalues are larger than the typical inter-eigenvalue separation, hence in the latter, the eigenvalues are essentially randomized over the dual circle on which the eigenvalues live. We will discuss this distinction in more detail in Section 5.

2.1 Relevant scales and two large- N_c limits: 't Hooft vs. Abelian

The gauge theory compactified on $\mathbb{R}^3 \times \mathbb{S}^1$ contains an extra parameter, the compactification scale L . Thus, if center symmetry remains unbroken at small L , the large- N_c limit is more

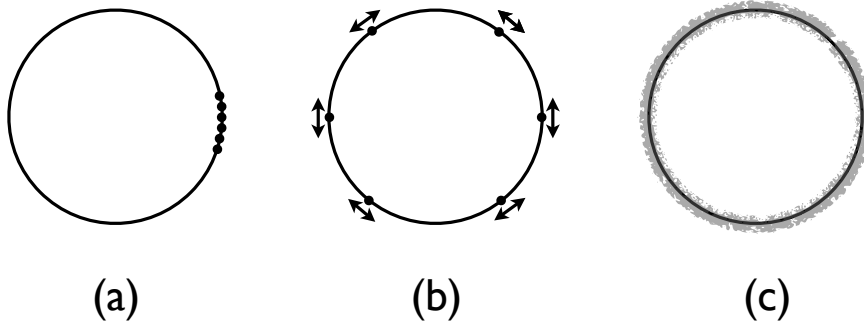


Figure 3: Three types of gauge holonomy: **a)**: Weak coupling trivial holonomy associated with deconfined phase. **b)**: Weak coupling non-trivial holonomy associated with the weak coupling confined phase. **c)**: Strong coupling non-trivial holonomy associated with the strong coupling confined phase. It is important to note that **b)** admits an adjoint-Higgs description, whereas **c)** does not. These two confinement regimes are continuously connected.

subtle than the standard 't Hooft limit.³ In fact, there are two large- N_c limits, which we refer to as the (naive) 't Hooft limit and the abelian limit. The reason that there is more than one limit is that m_W , the mass of the lightest off-diagonal gluon, goes to zero if the large- N_c limit is taken with LA fixed. This means that the effective abelian theory breaks down in the naive 't Hooft limit. When we study the large- N_c limit we will therefore consider the limit $N_c \rightarrow \infty$ with $m_W = 2\pi/(N_c L) = \text{const}$, i.e., $L = O(N_c^{-1})$. In other words, ensuring the validity of the weakly-coupled effective theory requires shrinking the size of the circle when taking the large- N_c limit. In what follows, we will express all dimensionful quantities in the effective lagrangian for the light modes on $\mathbb{R}^3 \times \mathbb{S}^1$ in terms of m_W and the scale parameter of the gauge theory, Λ , with the understanding that they are both fixed in the large- N_c limit,

$$\Lambda^3 = \mu^3 \frac{16\pi^2}{3N_c g^2(\mu)} \exp\left(-\frac{8\pi^2}{g^2(\mu)N_c}\right),$$

$$m_W = \frac{2\pi}{N_c L} \gg \Lambda. \quad (2.4)$$

The above expression for Λ is the standard 2-loop expression for the scale parameter [19]. Note that Ref. [6] uses a definition of Λ^3 that differs by a factor of proportional to N_c . The gaugino mass m introduces another length scale in the problem. The validity of the fermion zero mode induced pairing mechanism of bions requires that $m \ll g^2(m_W)/L$, the inverse bion size. In terms of the scales in Eq. (2.4), the gaugino mass should parametrically obey

$$m \ll \frac{m_W}{\log \frac{m_W}{\Lambda}}, \quad (2.5)$$

³This issue does not arise in thermal compactifications, and as a consequence it has not been discussed until recently, see [7].

an upper bound which remains finite in the large- N_c limit.

2.2 The bion and monopole potentials in softly-broken $SU(N_c)$ theory on $\mathbb{R}^3 \times \mathbb{S}^1$

Here, we describe the Lagrangian governing the long-distance dynamics of the $SU(N_c)$ gauge theories on $\mathbb{R}^3 \times \mathbb{S}^1_L$ for general N_c . The effective Lagrangian follows from the superpotential of Ref. [6] and the field redefinition in Eq. (2.1) in a rather straightforward way, generalizing the detailed derivation given in [1] for $N_c = 2$. The kinetic term of the light fields (2.1) is:⁴

$$\mathcal{L}_{kin.} = \frac{g^2(m_W)}{16\pi^2 L} \left((\partial_\mu \vec{b}')^2 + (\partial_\mu \vec{\sigma}')^2 \right), \quad (2.6)$$

where m_W is given in (2.4). The nonperturbative potential due to bions and monopole-instantons is:

$$\begin{aligned} V_{np}^{(k)} = & V_{bion}^0 \left[\sum_{i=1}^{N_c} e^{-2\vec{\alpha}_i \cdot \vec{b}'} - e^{-(\vec{\alpha}_i + \vec{\alpha}_{i+1}) \cdot \vec{b}'} \cos [(\vec{\alpha}_i - \vec{\alpha}_{i+1}) \cdot \vec{\sigma}'] \right] \\ & - V_{mon}^0 \left[\sum_{i=1}^{N_c} \left(1 + \frac{g^2 N_c}{8\pi^2} \vec{\alpha}_i \cdot \vec{b}' \right) e^{-\vec{\alpha}_i \cdot \vec{b}'} \cos \left(\vec{\alpha}_i \cdot \vec{\sigma}' + \frac{2\pi k + \theta}{N_c} \right) \right], \end{aligned} \quad (2.7)$$

where we have included the dependence on the θ parameter of the gauge group, which only contributes if the gaugino mass is nonzero. The parameter $k = 0, 1, \dots, N_c - 1$ labels the vacuum branch as in Eq. (2.1). The true effective potential corresponds to the branch that gives the minimum ground state energy, the other branches describe metastable vacua. These vacua are expected to become quasi-stable in the large- N_c limit [20]. The strengths of the bion and monopole potentials are given by

$$V_{bion}^0 = \frac{32\pi^2 L}{g^2(m_W)} \frac{\mu^6 L^2}{g^4(\mu)} \exp \left(-\frac{16\pi^2}{g^2(\mu) N_c} \right), \quad (2.8)$$

$$V_{mon}^0 = \frac{4Lm\mu^3}{g^2(\mu)} \frac{8\pi^2}{g^2(\mu) N_c} \exp \left(-\frac{8\pi^2}{g^2(\mu) N_c} \right). \quad (2.9)$$

For $N_c = 2$ and $\theta = 0$ the above result reduces to the expressions given in [1]. We can express these results in terms of the physical scales defined in Eq. (2.4). The kinetic term is

$$\mathcal{L}_{kin.} = \frac{1}{12\pi} \frac{m_W}{\log\left(\frac{m_W}{\Lambda}\right)} \left((\partial_\mu \vec{b}')^2 + (\partial_\mu \vec{\sigma}')^2 \right), \quad (2.10)$$

and the coefficients (2.8, 2.9) of the bion and monopole potentials are

$$V_{bion}^0 = \frac{27}{8\pi} \frac{\Lambda^6}{m_W^3} \log \left(\frac{m_W}{\Lambda} \right), \quad (2.11)$$

$$V_{mon}^0 = \frac{9}{2\pi} \frac{m\Lambda^3}{m_W} \log \left(\frac{m_W}{\Lambda} \right). \quad (2.12)$$

⁴The kinetic terms of \vec{b}' and $\vec{\sigma}'$ receive perturbative corrections along the Coulomb branch. These are closely related to the non-cancelling one-loop fluctuation determinants around supersymmetric instanton-monopole solutions on $\mathbb{R}^3 \times \mathbb{S}^1$. This subtlety is studied in detail in Appendix A of [1]. However, as in that reference, our results in the weakly-coupled calculable regime are unaffected to leading order.

For future use, we also introduce the dimensionless ratio of Eq. (2.12) and (2.11):

$$c_m = \frac{V_{mon}^0}{V_{bion}^0} = \frac{4mm_W^2}{3\Lambda^3} = \frac{16\pi^2 m}{3\Lambda(\Lambda L N_c)^2}. \quad (2.13)$$

We first study the spectrum in the limit when the supersymmetry breaking perturbation is turned off, $m = 0$. For this purpose we expand the bion potential to quadratic order in \vec{b}' and $\vec{\sigma}'$. Because of the exact supersymmetry the \vec{b}' and $\vec{\sigma}'$ masses are identical and we can concentrate on the \vec{b}' field. We rescale \vec{b}' to canonically normalize the kinetic term (2.10), and also drop the prime in the following. We find the following quadratic lagrangian

$$\mathcal{L} = \frac{1}{2}(\partial_\mu \vec{b})^2 + m_0^2 \sum_{i=1}^{N_c} \left[(\vec{\alpha}_i \cdot \vec{b})^2 - (\vec{\alpha}_i \cdot \vec{b}) (\vec{\alpha}_{i+1} \cdot \vec{b}) \right]. \quad (2.14)$$

with

$$m_0^2 = \frac{81 \Lambda^6 [\log(\frac{m_W}{\Lambda})]^2}{4 m_W^4}. \quad (2.15)$$

The mass term in (2.14) can be diagonalized by switching to $U(N_c)$ roots given by N_c -dimensional vectors of the form $\alpha_1 = (1, -1, 0, \dots)$, $\alpha_2 = (0, 1, -1, 0, \dots)$, etc., $\alpha_{N_c} = (-1, 0, \dots, 0, 1)$, see [21]. This introduces an extra massless particle that decouples from the rest of the spectrum. We get

$$\mathcal{L} = \frac{1}{2}(\partial_\mu \vec{b})^2 + \frac{1}{2} m_0^2 \sum_{i=1}^{N_c} (b_{i+2} - 2b_{i+1} + b_i)^2. \quad (2.16)$$

This is a simple lattice model that can be diagonalized by introducing \mathbb{Z}_{N_c} Fourier modes

$$b_j = \frac{1}{\sqrt{N_c}} \sum_{p=0}^{N_c-1} \tilde{b}_p e^{-2\pi i \frac{pj}{N_c}}. \quad (2.17)$$

The spectrum of the \vec{b} fields is

$$m_b = 4m_0 \sin^2 \left(\frac{p\pi}{N_c} \right) = 18\Lambda \frac{\Lambda^2 \log \frac{m_W}{\Lambda}}{m_W^2} \sin^2 \left(\frac{p\pi}{N_c} \right), \quad (p = 1, \dots, N_c - 1), \quad (2.18)$$

where we have dropped the unphysical massless mode $p = 0$ (which was introduced above via the transition to N_c -dimensional roots). From Eq. (2.18) we conclude that all the \vec{b} -fields are parametrically lighter than the W -bosons and that the effective theory is consistent in the large- N_c limit, see Eq. (2.4).

Let us now turn on the gaugino mass m . At first, we ignore the θ -dependence and take $\theta = 0$ and $k = 0$ (it is easy to see that for $\theta = 0$ the $k = 0$ vacuum in Eq. (2.1) has the minimal energy). In this vacuum, there is no mixing between the \vec{b}' and $\vec{\sigma}'$ fields when the monopole potential is expanded up to quadratic terms around their vanishing expectation values. In

the weak coupling limit $\frac{g^2 N_c}{8\pi^2} = [3 \log(m_W/\Lambda)]^{-1}$, so we can neglect the $g^2 N_c$ term in the monopole potential in Eq. (2.7). We now find, instead of (2.14), the quadratic Lagrangian

$$\mathcal{L} = \frac{1}{2}(\partial_\mu \vec{b})^2 + m_0^2 \sum_{i=1}^{N_c} \left[(\vec{\alpha}_i \cdot \vec{b})^2 - (\vec{\alpha}_i \cdot \vec{b}) (\vec{\alpha}_{i+1} \cdot \vec{b}) - \frac{c_m}{2} (\vec{\alpha}_i \cdot \vec{b})^2 \right]. \quad (2.19)$$

Thus, the monopole term is diagonal in the Fourier basis given in Eq. (2.17), and the only difference is that the quadratic part of the monopole potential has eigenvalues that are proportional to the square of $\sin(p\pi/N_c)$. The squared mass of the \vec{b} field as a function of m is

$$m_b^2 = 16m_0^2 \left\{ \left[\sin \left(\frac{p\pi}{N_c} \right) \right]^4 - \frac{c_m}{4} \left[\sin \left(\frac{p\pi}{N_c} \right) \right]^2 \right\}. \quad (2.20)$$

We observe that the center symmetric vacuum becomes locally unstable for $c_m > c_m^*$, where, taking $p = 1$, $c_m^* = 4 \sin^2(\frac{\pi}{N_c})$. This corresponds to $m > m^*$ with

$$m^* = \frac{3\Lambda^3}{m_W^2} \sin^2 \left(\frac{\pi}{N_c} \right) \xrightarrow{N_c \rightarrow \infty} \frac{3\pi^2 \Lambda^3}{N_c^2 m_W^2}. \quad (2.21)$$

for fixed L as one varies m . On the other hand, for fixed m , as one varies L , this implies a local instability at

$$L^* = \Lambda^{-1} \sqrt{\frac{4m}{3\Lambda}} \frac{1}{\frac{N_c}{\pi} \sin \frac{\pi}{N_c}} \xrightarrow{N_c \rightarrow \infty} \Lambda^{-1} \sqrt{\frac{4m}{3\Lambda}}. \quad (2.22)$$

It is clear that m^* (or L^*) is within the region of validity of the semi-classical approximation given in Eq. (2.5).

We note, however, that for any $N_c > 2$ the non-perturbative potential contains cubic terms. This implies that the transition is first order, and that c_m^* is not the critical coupling, but rather it is the limit of metastability above which the confining vacuum ceases to be a (local or a global) minimum. The critical mass, m_{cr} , is smaller than m^* in Eq. (2.21). We will determine the critical values of c_m^{cr} in Section 2.4. For $c_m^{cr} < c_m < c_m^*$ the center-symmetric minimum is a metastable local minimum but not the global minimum.

2.3 The perturbative potential for arbitrary N_c

Before we continue our study of the phase transition we will first show that the perturbative (Gross-Pisarski-Yaffe) contribution to the potential for the holonomy is sub-leading compared to the monopole and bion induced potentials, as in the $N_c = 2$ case. The perturbative potential for the Polyakov line in $SU(N_c)$ is

$$V_{pert} = -\frac{m^2}{L} \sum_{N_c \geq j > i \geq 1} B_2 \left(\frac{q_{ij}}{2} \right), \quad (2.23)$$

where we have neglected higher order terms in the mass of the adjoint fermion. Here, $B_2(x) = x^2 - x + 1/6$ is the Bernoulli polynomial of order 2, and

$$q_{ij} = \frac{2}{N_c}(j-i) + \frac{g^2}{4\pi} (b'_i - b'_j). \quad (2.24)$$

For small b'_i we can ignore the periodicity of the potential. The center symmetric point $b'_i = 0$ is a local *maximum* of the perturbative one-loop potential. At order m^2 the potential near the center symmetric vacuum is exactly quadratic,

$$V_{pert} = -\frac{m_{pert}^2}{2N_c} \sum_{j>i} (b_i - b_j)^2, \quad m_{pert}^2 = \frac{2m^2\pi^2}{3 \log(\frac{m_W}{\Lambda})}, \quad (2.25)$$

where we have dropped a constant term and normalized the kinetic term as in Eq. (2.14). The sum can be diagonalized in terms of the \mathbb{Z}_{N_c} Fourier modes given in Eq. (2.17). The tachyonic mass for the p 'th mode is

$$m_b^2 = -\frac{m_{pert}^2}{4N_c} \sum_{j>i} \left[\sin\left(\frac{\pi p(j-i)}{N_c}\right) \right]^2 = -m_{pert}^2, \quad (2.26)$$

independent of p . We can compare this result to bion generated mass of the lowest mode,

$$m_b^2 \sim \frac{\Lambda^6}{N_c^4 m_W^4} \left[\log\left(\frac{m_W}{\Lambda}\right) \right]^2. \quad (2.27)$$

At the critical mass m^* defined in equ. (2.21) the tachyonic mass is

$$m_b^2 \sim \frac{\Lambda^6}{N_c^4 m_W^4} \left[\log\left(\frac{m_W}{\Lambda}\right) \right]^{-1}, \quad (2.28)$$

and we conclude that the perturbative contribution is suppressed by three powers of $\log(m_W/\Lambda)$. This is the same suppression factor we found in $N_c = 2$ [1]. We will henceforth ignore the contribution of the perturbative fluctuations to the potential for the holonomy.

2.4 The phase transition and the limits of metastability for $N_c \geq 3$

In Section 2.2 we determined the limit of metastability c_m^* at which the origin of the effective potential for $N_c \geq 3$ becomes unstable, and the metastable phase disappears. In this section we will numerically determine the critical c_m^{cr} for the first order phase transition.

SU(3): For $N_c = 3$, one can plot the potential as a function of the deviation of the holonomies from their center symmetric values (i.e., b'_1, b'_2) for different values of c_m and observe the nature of the transition, see Figure 4. For $\theta = 0$, the expectation value of $\vec{\sigma}'$ remains zero. The critical value for the first order transition is $c_m^{cr} = 2.446$, see Figure 5.

For $c_m < c_m^{**}$, where c_m^{**} is one of the limits of metastability, there is a unique center-symmetric minimum (confining phase), see the left panel of Figure 4 as well as Figure 5. For $c_m^{**} < c_m < c_m^{cr}$, there is a center-symmetric global minimum (confined phase) and three center-broken metastable (deconfined) local minima (not shown in Figure 4, but shown in Figure 5). This also provides an alternative definition c_m^{**} . It is the value of c_m below which the metastable center-broken minima disappears, hence the name limit of meta-stability.

For $c_m^{cr} < c_m < c_m^*$, where $c_m^* = 3$ is the limit of metastability, the three \mathbb{Z}_3 breaking minima are global degenerate minima, and the center-symmetric confining phase is a local but

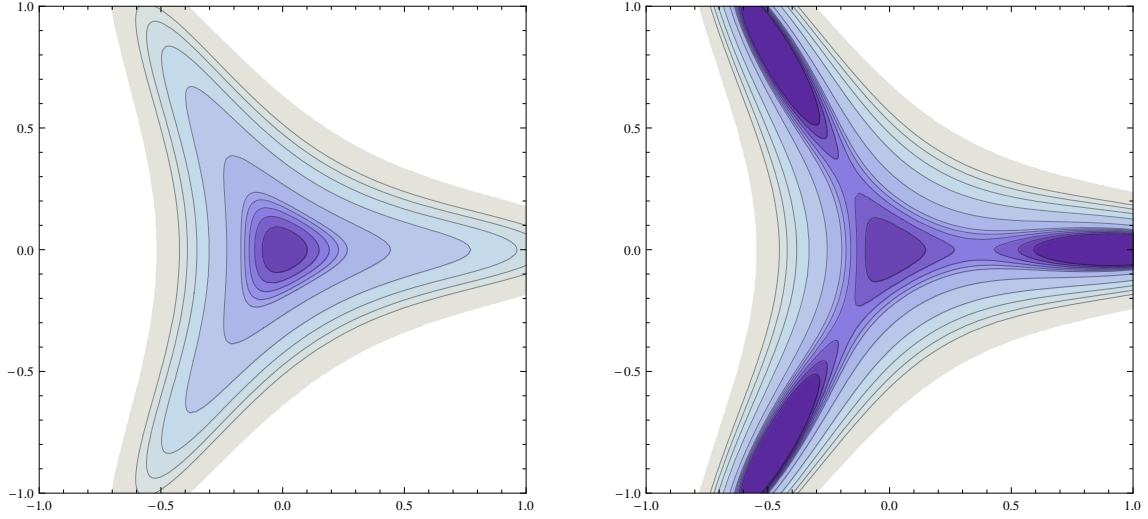


Figure 4: Contour plots of the bion- and monopole-instanton-induced potential, as a function of the two holonomies, showing the first order phase transition for $SU(3)$ (darker shades represent smaller values of the potential). Left panel: Contour plot for $c_m < c_m^{**} < c_m^{cr}$ ($c_m = 2.20$, $c_m^{cr} = 2.446$) as a function of b_1, b_2 . The \mathbb{Z}_3 -symmetric (confining) minimum is at the origin. Right panel: Contour plot for $c_m^{cr} < c_m < c_m^*$ ($c_m = 2.5$) as a function of b_1, b_2 . The \mathbb{Z}_3 -breaking global minima are clearly visible, and the \mathbb{Z}_3 -symmetric confining minimum is meta-stable.

not a global minimum, see the right panel of Figure 4. In this regime the confining phase is meta-stable. Finally, for $c_m > c_m^*$, the center-symmetric point ceases to be a local minimum, and this correspond to the other limit of metastability. This case is not shown in Figure 4, but shown in Figure 5.

$SU(N_c), N_c > 3$: The general structure that emerges for $SU(N_c), N_c > 3$ is similar to the $SU(3)$ case shown in Figure 5. We have four characteristic domains for the bion and monopole-instanton induced potential:

- $c_m < c_m^{**}$ or $L > L^{**}$: There is a unique center-symmetric (confined) minimum.
- $c_m^{**} < c_m < c_m^{cr}$ or $L^{**} > L > L^{cr}$: A global center-symmetric (confined) minimum and N_c meta-stable \mathbb{Z}_{N_c} breaking (deconfined) minima.
- $c_m^{cr} < c_m < c_m^*$ or $L^{cr} > L > L^*$: A metastable center-symmetric (confined) minimum and N_c global \mathbb{Z}_{N_c} breaking (deconfined) minima.
- $c_m^* < c_m$ or $L^* > L$: N_c center-breaking global (deconfined) minima.

A lattice study of the endpoint of the regime of metastability in pure Yang-Mills theory was reported in [22]. This study was motivated by the old idea that in large- N_c QCD the

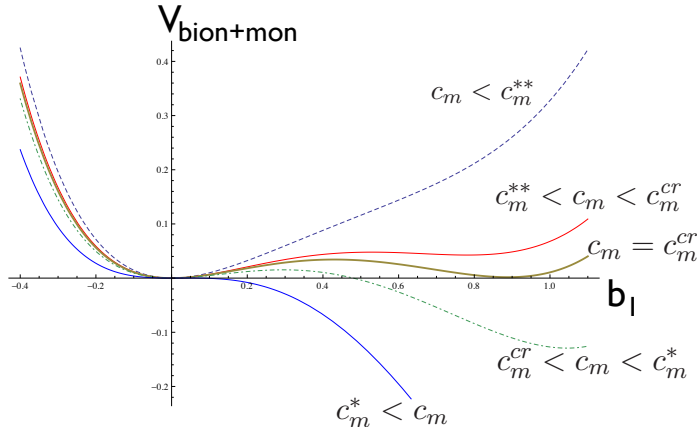


Figure 5: Effective potential due to bions and monopoles for different values of c_m . The potential (in units of V_{bion}^0) is shown as a function of b_1 for $b_2 = 0$, corresponding to a cut along the x -axis in Fig. 4.

Hagedorn temperature T_H , the limiting temperature of a hadronic resonance gas, must correspond to a second order phase transition which occurs above the (first order) deconfining transition [23–25]. The regime $T_c < T < T_H$ is therefore metastable. This behavior was also observed in large- N_c theories compactified on $S^3 \times S^1$ [26, 27].

For $N_c > 3$ the potential is a function of $N_c - 1$ holonomies. Instead of trying to plot this function we will study the vacuum expectation values of the N_c eigenvalues of the Wilson line around \mathbb{S}^1 as a function of the gaugino mass parameter c_m . We will, again, observe a discontinuous transition, which occurs at values of c_m^{cr} smaller than the c_m^* given in (2.21). The eigenvalue repulsion due to the neutral (center-stabilizing) bions is dominant at small c_m and is, upon increasing c_m , countered by the eigenvalue attraction due to monopole-instantons along with the one-loop potential which is sub-leading, see Section 2.3. We plot the eigenvalues of Ω as c_m^{cr} is crossed. We show the behavior of the eigenvalue distributions for $N_c = 4, 5$, and 10 in Figures 6, 7, and 8, respectively. In order to make these plots we chose a specific value of the 't Hooft coupling, $g^2 N_c = 0.1$. The critical value c_m^{cr} is independent of the coupling constant in the weak coupling limit. Results for c_m^* and c_m^{cr} are compiled in Table 2.

The discontinuity at the first order phase transition can be quantified in terms of the change in the trace of the Wilson line. In weak coupling, $g^2 N_c / (4\pi) \ll 1$, we have

$$\text{tr}\langle\Omega\rangle \approx i \left(\frac{g^2 N_c}{4\pi} \right) \frac{1}{N_c} \text{tr} \left(\Omega_0 \vec{H} \cdot \langle \vec{b}' \rangle \right), \quad (2.29)$$

where $\Omega_0 = e^{i \frac{2\pi}{N_c} \vec{H} \cdot \vec{\rho}}$ is the center-symmetric holonomy. The discontinuity $\Delta|\text{tr}\langle\Omega\rangle|$ at c_m^{cr} , calculated from Eq. (2.29) using the numerical value for c_m^{cr} , is also given in Table 2. The data for the discontinuity of the trace (with maximal trace normalized to unity) can be

N_c	$c_m^* = 4 \sin^2 \frac{\pi}{N_c}$	c_m^{cr}	$\frac{N_c^2}{4\pi^2} \times c_m^{cr}$	$\Delta \text{tr}\langle\Omega\rangle \times \left(\frac{4\pi}{g^2 N_c}\right)$
3	3.000	2.45	0.56	0.37
4	2.000	1.47	0.60	0.57
5	1.382	0.97	0.61	0.75
6	1.000	0.68	0.62	0.91
7	0.753	0.50	0.62	1.07
8	0.586	0.38	0.61	1.22
9	0.467	0.30	0.61	1.37
10	0.382	0.24	0.61	1.53

Table 2: Critical values c_m^* and c_m^{cr} for the endpoint of the metastable phase and the first order transition in $SU(N_c)$ gauge theory with one adjoint fermion on $\mathbb{R}^3 \times \mathbb{S}_1$. We also show the critical coupling c_m^{cr} scaled by $4\pi^2/N_c^2$, and give the discontinuity of the Wilson line in the weak coupling limit.

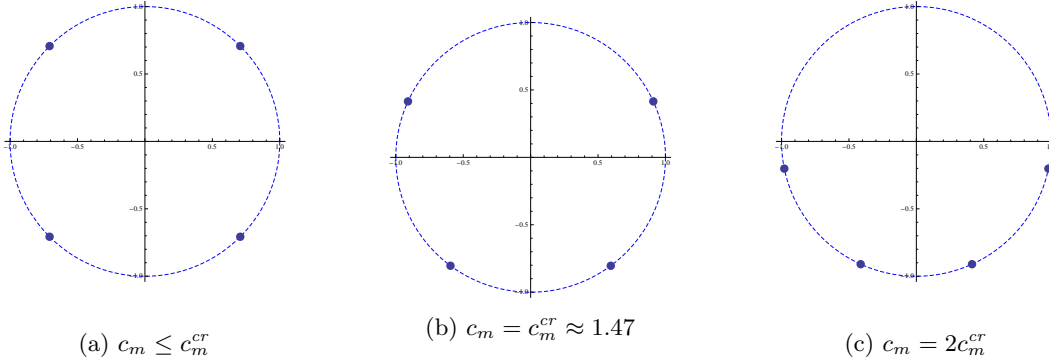


Figure 6: The distribution of the eigenvalues of the Polyakov loop around \mathbb{S}_L^1 for $N_c = 4$ for different values of c_m , shown for $g^2 N_c = 0.1$.

represented by the expression

$$\Delta \left| \frac{1}{N_c} \text{tr}\Omega \right| \simeq \left(0.163 - \frac{0.085}{N_c} \right) \frac{g^2 N_c}{4\pi}, \quad (2.30)$$

which is valid in the large- N_c limit with the parameters given in Eq. (2.4) held fixed.

2.5 More on the (abelian) large- N_c limit and (evading) the Hagedorn instability

So far, we have computed the critical mass numerically for $N_c = (3, 4, \dots)$. The numerical results indicate that the critical value of the gaugino mass, m_{cr} , is equal to m_* up to a factor of order one for arbitrary N_c . This can be seen from the fourth column of Table 2, which shows the value of c_m^{cr} scaled by the asymptotic value of c_m^* . Therefore, using Eq. (2.21, 2.22), we observe that $\frac{m_*}{\Lambda} \sim \frac{3}{4}(L\Lambda)^2$ at fixed L , or $L^* \sim \Lambda^{-1} \sqrt{\frac{4m}{3\Lambda}}$ at fixed m . We conclude that in the scaling regime the $SU(2)$ result derived in [1] has a smooth large- N_c limit.

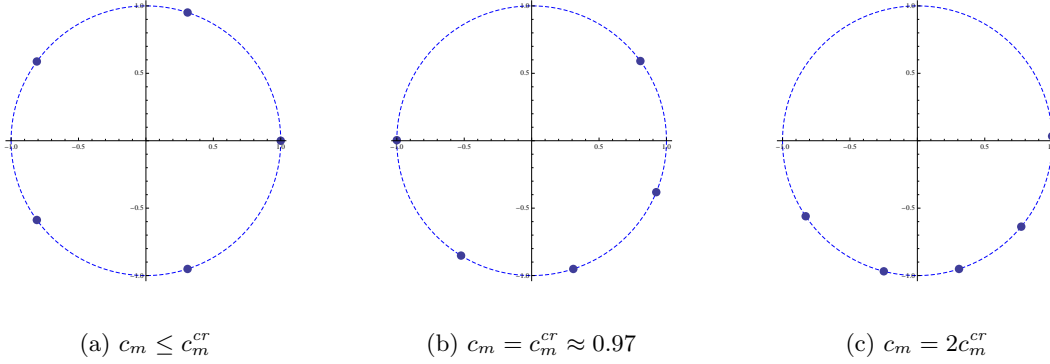


Figure 7: The distribution of the eigenvalues of the Polyakov loop around \mathbb{S}_L^1 for $N_c = 5$ for different values of c_m , shown for $g^2 N_c = 0.1$.

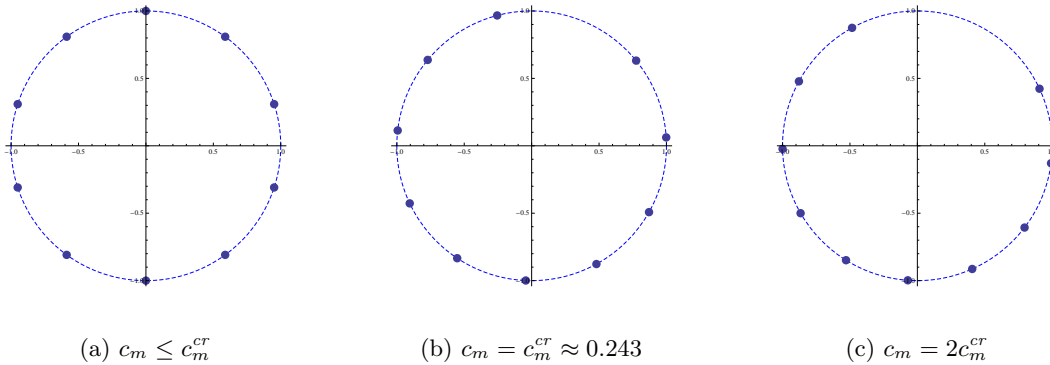


Figure 8: The distribution of the eigenvalues of the Polyakov loop around \mathbb{S}_L^1 for $N_c = 10$ for different values of c_m , shown for $g^2 N_c = 0.1$.

We note that in the abelian confinement regime the size of the dual circle $\tilde{\mathbb{S}}^1$ on which the eigenvalues reside is equal to $1/L$, which grows linearly with N_c , while the separation of the eigenvalues remains fixed, $2\pi/(LN_c) \sim O(N_c^0)$. This is in sharp contrast with the non-abelian confinement regime and the ordinary large- N_c limit. In the latter, $1/L = O(N_c^0)$ and the separation between eigenvalues is $2\pi/(LN_c) \sim O(N_c^{-1})$, forming a dense set in perturbation theory. In the latter case, since $2\pi/(LN_c) \ll \Lambda$, all the low momentum modes are strongly coupled, and the eigenvalues are uniformly distributed over the unit circle. At the critical point in the weakly coupled regime, the uniform separation between eigenvalues exhibits a jump into a non-uniform one, by opening a “gap” on top of the usual one. As one increases c_m the gap continues to grow, as shown in Figures 6, 7, and 8 for $SU(4)$, $SU(5)$, and $SU(10)$, respectively. In particular, we did not observe, in the semi-classical regime, an instability towards partial center-symmetry breaking phases, similar to those found in deformed Yang-Mills theory and massive QCD(adj), [7, 28], see Ref. [29] for a review.

There is one more interesting issue that appears in the large- N_c limit. The density of states of large- N_c gauge theories is expected to exhibit an exponential growth, $\rho(E) \sim e^{\beta^* E} = e^{E/T_H}$, where $\beta^* \equiv T_H$ is the Hagedorn temperature. This idea is related to the

conjecture that large- N_c gauge theory is dual to a weakly coupled string theory whose density of states is known to grow exponentially. Then, $Z(\beta) = \int^\infty dE e^{(\beta^* - \beta)E}$ diverges for $\beta < \beta^*$, indicating the existence of a limiting temperature for the confined phase. As discussed above T_H is expected to be larger than T_c . In simulations of $SU(12)$ Yang-Mills it was found that $T_H = 1.116T_c$ [22]. This seems to imply that it is impossible to extend the confined phase to the regime of small- L and weak coupling. Naively, even if one evades deconfinement, it seems unlikely that one can evade the Hagedorn instability. It is noteworthy to understand how our construction avoids this obstacle.

The bosonic and fermionic density of states $\rho_{\mathcal{B}}(E)$ and $\rho_{\mathcal{F}}(E)$ are properties of the Hamiltonian, independent of the boundary condition along the \mathbb{S}_1 . The crucial point is that the density operator $e^{-\beta H}$ of the thermal compactification is replaced by a \mathbb{Z}_2 -graded density operator, $e^{-\beta H}(-1)^F$, whose matrix elements, unlike the ordinary density matrix, are not necessarily positive definite. The twisted partition function is of the form $\tilde{Z}(L) = \int^\infty dE (\rho_{\mathcal{B}}(E) - \rho_{\mathcal{F}}(E))e^{-LE}$, so that even if the density of states grows exponentially the spatially compactified theory need not have a limiting scale. This is most transparent in the supersymmetric limit, where all positive energy states are paired bosonic and fermionic states, and $\tilde{Z}(L)$ is the supersymmetric index.⁵ In the softly broken supersymmetric theory, we find a phase transition at the scale given in Eq. (2.22), $L^* \sim \Lambda^{-1} \sqrt{\frac{m}{\Lambda}} \ll \frac{2\pi}{\Lambda N_c}$ (recall (2.4)), parametrically smaller than the Hagedorn scale $\beta^* \sim \Lambda^{-1}$. Strictly speaking, this is a quantum phase transition, which should not be interpreted thermally for small m . However, it is continuously connected to the thermal deconfinement transition, and this makes the semi-classical analysis feasible.

3. θ -dependence of the phase transition and topological interference

In the Minkowski-space formulation of the path integral, the θ -term generates an extra phase of the path amplitude, $e^{iS(\gamma)} \rightarrow e^{iS(\gamma) + i\theta Q(\gamma)}$, where γ is the path connecting the initial and final field configurations. This is analogous to the Aharonov-Bohm (AB) phase in quantum mechanics, and the θ -angle can be viewed as an AB-flux. Turning on the θ angle generates interference among path amplitudes which affects physical observables and the vacuum structure of the theory.

In the case of Yang Mills theory analytic continuation of the path integral to Euclidean space induces a positive definite action for $\theta = 0$. However, for $\theta \neq 0$, the theory has a sign problem, preventing straightforward numerical simulations, see Ref. [30, 31] and references therein. In the semi-classical regime the sign problem manifests itself as a complex fugacity for topological configurations. For example, the 4d instanton fugacity e^{-S_I} is modified to $e^{-S_I + i\theta}$. The density of topological configurations remain unaltered, but they acquire a pure phase depending on the topological charge. This leads to qualitative and quantitative changes

⁵These considerations are not restricted to supersymmetry theories, or theories with softly broken supersymmetry. For example, $N_c = \infty$ non-supersymmetric QCD with multiple adjoint fermions does not possess *any* phase transition upon circle compactification, and satisfies large- N_c volume independence, see [7, 18] and references therein.

in the vacuum structure of the theory, which we refer to as *topological interference* effects. In particular, the fugacity of 1-defects (monopole-instantons) becomes complex, but the fugacity of topologically neutral bions remains unchanged. In the case of magnetic bions the result depends on the gauge group G — for $SU(N_c)$ the fugacity remains unaltered, but for G_2 it acquires a phase depending on the topological charge of the magnetic bion.

There is a subtle point here (for an earlier related discussion, see [32]). The action of the monopole-instanton is modified as $\exp(-S_0) \rightarrow \exp(-S_0 + \frac{i\theta}{N_c})$ with $S_0 = 8\pi^2/(g^2 N_c)$. Since θ is a periodic variable with period 2π , this implies that there exists a family of Lagrangians:

$$\mathcal{L}^{(k)} = \mathcal{L}_{kin.} + V_{np}^{(k)}, \quad k = 0, \dots, N_c - 1 \quad (3.1)$$

where the N_c potentials $V_{np}^{(k)}$ are given in Eq. (2.7), and the kinetic term $\mathcal{L}_{kin.}$ in Eq. (2.10). For a given value of θ , we must determine the correct effective long-distance theory. The correct theory is determined by comparing the vacuum energy density associated with each branch, and selecting the branch with the minimum vacuum energy. The theta dependence of the vacuum energy density, at leading order in semi-classical expansion, is given by

$$\mathcal{E}(\theta) = \min_k \mathcal{E}_k(\theta) \equiv \min_k \left[-\frac{V_{mon}^0}{L} \cos\left(\frac{2\pi k + \theta}{N_c}\right) \right], \quad (3.2)$$

which arises from monopole-instantons. The contribution due to neutral and magnetic bions cancel each other exactly, and the analytic contribution of 4d instantons is exponentially suppressed. Eq. (3.2) implies that the vacuum energy is analytic everywhere except for odd integer multiples of π where it exhibits non-analyticity. For example, in the range $\theta \in (-\pi, \pi)$ the ground state energy density is $\mathcal{E}_0(\theta)$, while for $\theta \in (\pi, 3\pi)$ the vacuum energy density is $\mathcal{E}_1(\theta)$. This implies that at $\theta = \pi$ the $k = 0$ and $k = 1$ branches become degenerate. This degeneracy that we see in the long-distance effective theory is a manifestation of the CP-symmetry in the microscopic theory at $\theta = \pi$. Thus, the vacuum structure and the symmetry realization for general group G is modified at $\theta = \pi$ as

$$\theta = \pi : \quad Z(G) \times Z_2^{\text{CP}} \implies \begin{cases} Z(G) \times 1 & \text{confined} \\ 1 \times Z_2^{\text{CP}} & \text{deconfined} \end{cases} \quad (3.3)$$

For all gauge groups, due to spontaneous breaking of CP, the vacuum in the confined phase is two-fold degenerate at $\theta = \pi$. Note that Z_2^{CP} also gives a symmetry that can be used to distinguish the phases of G_2, F_4, E_8 at $\theta = \pi$. At very high T , CP is restored and at low T it is broken.

Using Eq. (3.1), we can investigate the θ dependence for general observables, in particular the dependence of the phase transition and the critical scale on θ . It is not hard to see that the theta dependence is most pronounced for gauge groups of small rank. We first consider the case of $SU(2)$. We will show that $L^*(\theta)$ assumes its maximum at $\theta = \pi$, where the monopole-instantons events interfere destructively, resulting in a larger L^{cr} for breaking of the center symmetry. In the limit where the rank is large, T_c becomes theta independent.

3.1 θ -dependence of c_m^{cr} for $N_c = 2$

In the case $N_c = 2$ the θ -dependence of c_m^{cr} can be studied quite explicitly (the $N_c > 2$ case was recently studied in [34]). We take the $SU(2)$ roots as $\alpha_1 = -\alpha_2 = \sqrt{2}$ and find, from the potential given in Eq. (2.7):

$$\begin{aligned} \frac{V(b', \sigma')}{V_{bion}^0} &= 2 \cosh(2\sqrt{2}b') - 2 \cos(2\sqrt{2}\sigma') \\ &\quad - c_m \left(1 + \frac{g^2}{4\pi^2} \sqrt{2}b' \right) e^{-\sqrt{2}b'} \cos\left(\sqrt{2}\sigma' + \frac{\theta}{2} + \pi k\right) \\ &\quad - c_m \left(1 - \frac{g^2}{4\pi^2} \sqrt{2}b' \right) e^{\sqrt{2}b'} \cos\left(\sqrt{2}\sigma' - \frac{\theta}{2} - \pi k\right), \end{aligned} \quad (3.4)$$

where the various factors of $\sqrt{2}$ are due to the periodicities given in Eq. (2.2) and the normalization of the roots. Note that $k = 0, 1$ labels the choice of supersymmetric vacuum, corresponding to $\mathbb{Z}_4 \rightarrow \mathbb{Z}_2$ R -symmetry breaking. There is no R -symmetry when c_m is non-zero, and the vacuum branch is the $k = 0$ one when $\theta \in (-\pi, \pi)$. For the angular range $\theta \in (\pi, 3\pi)$, the vacuum branch is $k = 1$. Thus, proceeding with $k = 0$ and considering subcritical c_m , we find that for $\theta < \pi$ the global minimum of Eq. (3.4) is at $\langle \sigma \rangle = 0$, $\langle b' \rangle = 0$. For $\theta > \pi$ it is located at $\langle \sigma \rangle = \frac{\pi}{\sqrt{2}}$, $\langle b' \rangle = 0$, while for $\theta = \pi$ the two minima are degenerate, and the theory spontaneously violates CP.

Consider the range $0 \leq \theta \leq \pi$ (similar arguments apply to other values of θ). Expanding the potential to quadratic order around the minimum $\langle \sigma \rangle = 0$, $\langle b' \rangle = 0$ gives

$$8(\delta b \ \delta \sigma) \left[\begin{pmatrix} 1 & 0 \\ 0 & 1 \end{pmatrix} - \frac{c_m}{4} \begin{pmatrix} \left(1 - \frac{g^2}{2\pi^2}\right) \cos \frac{\theta}{2} & \left(1 - \frac{g^2}{4\pi^2}\right) \sin \frac{\theta}{2} \\ \left(1 - \frac{g^2}{4\pi^2}\right) \sin \frac{\theta}{2} & -\cos \frac{\theta}{2} \end{pmatrix} \right] \begin{pmatrix} \delta b \\ \delta \sigma \end{pmatrix}. \quad (3.5)$$

One of the two eigenvalues of the matrix inside the square brackets in Eq. (3.5) can change sign:

$$1 \pm \frac{c_m}{4} \left(1 - \frac{g^2}{4\pi^2} \left(1 \mp \cos \frac{\theta}{2} \right) \right), \quad (3.6)$$

where the signs are correlated. Thus, a negative eigenvalue appears at the critical value c_m^* . Extending the angular range to arbitrary θ ,

$$c_m^* = \max_{k=0,1} \left[4 + \frac{g^2}{\pi^2} \left(1 + \cos \left(\frac{\theta}{2} + \pi k \right) \right) + \dots \right], \quad (3.7)$$

where ellipsis represent terms with additional g^2 -suppression. Note that within the calculable regime, the critical c_m given in Eq. (3.7) only acquires θ dependence due to the g^2 -suppressed terms. This is special to the $N_c = 2$ case, for $N_c \geq 3$, θ dependence appear at the leading order.

Using (3.7), we obtain, like vacuum energy density or any other non-perturbative observable, a multi-branched function, which is two-branched for $SU(2)$, given by

$$L^*(\theta) = \min_{k=0,1} L_k^*(\theta) = L^*(0) \min_{k=0,1} \left[4 + \frac{g^2}{\pi^2} \left(1 + \cos \left(\frac{\theta}{2} + \pi k \right) \right) + \dots \right]^{-\frac{1}{2}}, \quad (3.8)$$

Both $L_0^*(\theta)$ and $L_1^*(\theta)$ are 4π periodic, whereas the $\min_{k=0,1} L_k^*(\theta)$ is 2π periodic as it must.

The physical interpretation of the two branches is as follows. For a given value of θ the potential in Eq. (3.4) always has two extrema. Both of these extrema are center-symmetric minima for small g and are located at $\langle\sigma\rangle = 0, \frac{\pi}{\sqrt{2}}$. For $\theta \neq \pi$, one of these minima is the true vacuum, say $k = 0$ and the other is meta-stable, say $k = 1$. $L_0^*(\theta)$ and $L_1^*(\theta)$ are the respective transition scales obtained by studying the theory on true vacuum versus meta-stable vacuum. At $\theta = \pi$, the two vacua become degenerate, leading to a cusp (non-analyticity) in $L^*(\theta)$, where $L_0^*(\theta) = L_1^*(\theta)$.

As Eq. (3.7) shows, as θ increases away from zero to π , the critical c_m^{cr} decreases. At fixed m decreasing c_m^{cr} implies increasing L^{cr} in the range $\theta \in [0, \pi)$. As in [33], the increase of L^{cr} with increasing θ can be attributed to “topological interference”. In our context, the physics of topological interference is that the effect of monopole-instantons is suppressed at $\theta = \pi$ with respect to $\theta = 0$ by destructive interference among path histories. As in Aharonov-Bohm phase, this extra topological phase factor gives additional interference among path histories (either Euclidean or Minkowski). Therefore, at $\theta = \pi$, the center-destabilizing potential due to monopole-instantons is suppressed with respect to $\theta = 0$. Comparing $\theta = \pi$ to $\theta = 0$ it requires stronger coupling, meaning a larger value of L , in order for the monopole-instantons to overcome the center-stabilizing (θ -independent) effect of the neutral bions.

If the weak coupling behavior holds qualitatively at strong coupling (i.e., for decoupling values of the gaugino mass), an increasing $L^{cr}(\theta)$ ($\beta^{cr}(\theta)$) implies that the deconfinement temperature $T_c(\theta)$ decreases with increasing $\theta \in [0, \pi]$. This behavior was discussed in [33] and recently observed in lattice simulations [30].

4. G_2 : First order transition without symmetry breaking

G_2 Yang Mills theory is an interesting test case for studying the deconfinement transition [35–41]. G_2 , along with F_4 and E_8 , has no global (center) symmetry and hence no obvious order parameter for deconfinement. Lattice calculations show that there is a first order phase transition between a low temperature “confined” phase, and a high temperature “deconfined” phase. In the confined phase there is an effective string potential at intermediate distances, but at very large distance the potential between fundamental charges is screened. The Wilson line is small but non-zero in the confined phase, and changes discontinuously at the phase transition. In the high temperature phase the Wilson line is close to one.⁶

The group G_2 has rank two. The fundamental representation is seven dimensional, and the adjoint representation has dimension 14. The tensor product of three 14 dimensional representations contains the fundamental representation, $[14] \times [14] \times [14] = [1] + [7] + \dots$, which explains why fundamental charges are screened. As in $SU(N_c)$ SYM theory on $\mathbb{R}^3 \times \mathbb{S}^1$ dynamical abelianization, $G_2 \rightarrow U(1)^2$, is a consequence of the existence of neutral bions,

⁶As discussed above the theory has a global \mathbb{Z}_2 (CP)symmetry at $\theta = \pi$. This symmetry is broken in the confined phase. It is easy to show that it is unbroken in the very high- T deconfined phase. However, it is not a priori obvious that CP restoration and the discontinuity of the Wilson line occur at the same critical temperature.

which generate a repulsion among the eigenvalues of Wilson line, see Fig. 9.⁷ The long distance theory contains the two dual photons $\vec{\sigma}$, their scalar superpartners $\vec{\phi}$ (the massless components of the gauge field along the \mathbb{S}^1), and fermionic superpartners.⁸ The fundamental Wilson line along \mathbb{S}^1 is

$$\Omega = e^{i\vec{H}\cdot\vec{\phi}}. \quad (4.1)$$

Similar to the $SU(N_c)$ case, we define the fluctuations \vec{b}' and $\vec{\sigma}'$ of the fields $\vec{\phi}$ and $\vec{\sigma}$ around the k -th supersymmetric ground state

$$\begin{aligned} \vec{\phi} &= \left(\frac{\pi}{2} + \frac{g^2}{16\pi} \log \frac{4}{3} \right) \vec{\rho} - \frac{g^2}{4\pi} (\vec{\omega}_1 \log 2 - \vec{\omega}_2 \log 3) + \frac{g^2}{4\pi} \vec{b}' \\ \vec{\sigma} + \frac{\theta \vec{\phi}}{2\pi} &= \frac{\theta + 2\pi k}{4} \vec{\rho} + \vec{\sigma}'. \end{aligned} \quad (4.2)$$

Here $k = 1, 2, 3, 4$ corresponds to a choice of vacuum breaking the discrete R symmetry of the supersymmetric theory, $\mathbb{Z}_8 \rightarrow \mathbb{Z}_2$. One difference from the $SU(N_c)$ case is that the expectation value of the fundamental Wilson loop Eq. (4.1) in the supersymmetric ground state $\langle \vec{\sigma}' \rangle = \langle \vec{b}' \rangle = 0$ is nonzero:

$$\begin{aligned} \text{tr}\langle \Omega \rangle &= \text{tr} e^{i\frac{\pi}{2}\vec{H}\cdot\vec{\rho} + i\frac{g^2}{4\pi}\vec{H}\cdot(\frac{1}{4}\vec{\rho}\log\frac{4}{3} - \vec{\omega}_1\log 2 + \vec{\omega}_2\log 3)} \\ &\approx \text{tr} e^{i\frac{\pi}{2}\vec{H}\cdot\vec{\rho}} \left(1 + i\frac{g^2}{4\pi}\vec{H}\cdot\left(\frac{1}{4}\vec{\rho}\log\frac{4}{3} - \vec{\omega}_1\log 2 + \vec{\omega}_2\log 3\right) \right) \\ &= \frac{g^2}{4\pi} \left(\frac{\pi \log 2}{\sqrt{3}} - \frac{\pi \log 3}{2} \right) \approx -0.15 \frac{g^2}{4\pi}. \end{aligned} \quad (4.3)$$

This should not come as a surprise, as there is no center symmetry requiring $\text{tr}\langle \Omega \rangle = 0$ in the confining phase.

The nonperturbative potential for the \vec{b}' and $\vec{\sigma}'$ is due to neutral bions, magnetic bions, and monopole-instantons. The result can be derived using the methods introduced in [1], based on the non-perturbative superpotential given in [6] and the field redefinition in Eq. (4.2).

⁷In phenomenological models it is straightforward to generate eigenvalue repulsion in $SU(N_c)$, but it is not easy to find a non-perturbative potential that leads to eigenvalue repulsion in G_2 , see Section VIII.C in [41]. We find that the neutral bion potential automatically gives eigenvalue repulsion for all gauge groups.

⁸The dual simple roots $\vec{\alpha}_1^*$, $\vec{\alpha}_2^*$, and the affine root $\vec{\alpha}_0^* = -2\vec{\alpha}_1^* - \vec{\alpha}_2^*$ (two dimensional vectors) have length squared 2 ($\vec{\alpha}_1^*$), 6 ($\vec{\alpha}_2^*$), and 2 ($\vec{\alpha}_0^*$), and obey $\vec{\alpha}_1^* \cdot \vec{\alpha}_2^* = -3$, $\vec{\alpha}_1^* \cdot \vec{\alpha}_0^* = -1$, $\vec{\alpha}_2^* \cdot \vec{\alpha}_0^* = 0$. The fundamental weights $\vec{\omega}_j$ obey $\vec{\omega}_i \cdot \vec{\alpha}_j^* = \delta_{ij}$ ($i, j = 1, 2$). The Weyl vector $\vec{\rho} = \vec{\omega}_1 + \vec{\omega}_2$ satisfies $\vec{\rho} \cdot \vec{\alpha}_{1,2}^* = 1$. The fundamental representation Cartan generators are normalized as $\text{tr}H_a H_b = 2\delta_{ab}$ and are explicitly given by $H_1 = \frac{1}{\sqrt{2}}\text{diag}(1, -1, 0, -1, 1, 0, 0)$, $H_2 = \frac{1}{\sqrt{6}}\text{diag}(1, 1, -2, -1, -1, 2, 0)$.

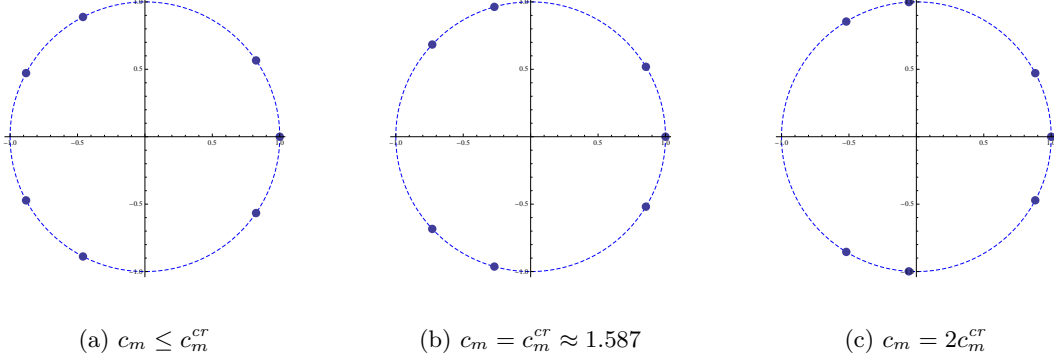


Figure 9: The distribution of the eigenvalues of the Polyakov loop around \mathbb{S}_L^1 for a G_2 gauge theory, for subcritical, critical, and supercritical values of c_m (plotted with $\frac{g^2}{4\pi} = 0.2$ in order to visualize the jump).

We find

$$\begin{aligned}
\frac{V_{total}}{V_{bion}^0} &= 4e^{-2\vec{b}' \cdot \vec{\alpha}_1^*} + 3e^{-2\vec{b}' \cdot \vec{\alpha}_2^*} + e^{-2\vec{b}' \cdot \vec{\alpha}_0^*} \\
&\quad - 6e^{-\vec{b}' \cdot (\vec{\alpha}_1^* + \vec{\alpha}_2^*)} \cos(\vec{\alpha}_1^* - \vec{\alpha}_2^*) \cdot \vec{\sigma}' - 2e^{-\vec{b}' \cdot (\vec{\alpha}_0^* + \vec{\alpha}_1^*)} \cos(\vec{\alpha}_0^* - \vec{\alpha}_2^*) \cdot \vec{\sigma}' \\
&\quad - c_m \left\{ \left(2 + \frac{g^2}{2\pi^2} \left(2\vec{b}' \cdot \vec{\alpha}_1^* - \frac{1}{2} \log 12 \right) \right) e^{-\vec{b}' \cdot \vec{\alpha}_1^*} \cos \left(\vec{\sigma}' \cdot \vec{\alpha}_1^* + \frac{\theta + 2\pi k}{4} \right) \right. \\
&\quad + \left(1 + \frac{g^2}{2\pi^2} \left(\vec{b}' \cdot \vec{\alpha}_2^* + \frac{1}{4} \log 108 \right) \right) e^{-\vec{b}' \cdot \vec{\alpha}_2^*} \cos \left(\vec{\sigma}' \cdot \vec{\alpha}_2^* + \frac{\theta + 2\pi k}{4} \right) \\
&\quad \left. + \left(1 + \frac{g^2}{2\pi^2} \left(\vec{b}' \cdot \vec{\alpha}_0^* - \frac{1}{4} \log \frac{3}{4} \right) \right) e^{-\vec{b}' \cdot \vec{\alpha}_0^*} \cos \left(\vec{\sigma}' \cdot \vec{\alpha}_0^* + \frac{\theta + 2\pi k}{4} \right) \right\}. \quad (4.4)
\end{aligned}$$

Similar to the $SU(N_c)$ case, we use V_{bion}^0 to denote the overall strength of the bion potential, while c_m is the ratio of the strengths of monopole to bion potentials. These parameters are given by

$$V_{bion}^0 = \frac{16\pi^2 \sqrt{3}}{g^2} L^3 \Lambda^6, \quad c_m = \frac{m}{L^2 \Lambda^3} \frac{1}{2^{\frac{3}{2}} 3^{\frac{1}{4}}}, \quad (4.5)$$

where

$$\Lambda^3 \equiv \frac{\mu^3}{g^2(\mu)} e^{-\frac{2\pi^2}{g^2(\mu)}} \quad (4.6)$$

is the scale parameter of G_2 Yang Mills theory, and the explicit factors of g^2 are normalized at the scale $m_W \sim 1/L$.

Let us now explain the origin of the various terms in V_{total} . Consider first the supersymmetric case $c_m = 0$, when the potential is given by the first two lines in Eq. (4.4). The terms independent of the dual photon $\vec{\sigma}'$ are due to the three kinds of center-stabilizing bions. The terms on the second line are due to magnetic bions, which come in two kinds only (because $\alpha_3^* \cdot \alpha_2^* = 0$). Magnetic bions are responsible for the generation of the mass gap of the dual photons and for confinement. It is easy to check that for $\vec{\sigma}' = \vec{b}' = 0$ the supersymmetric part

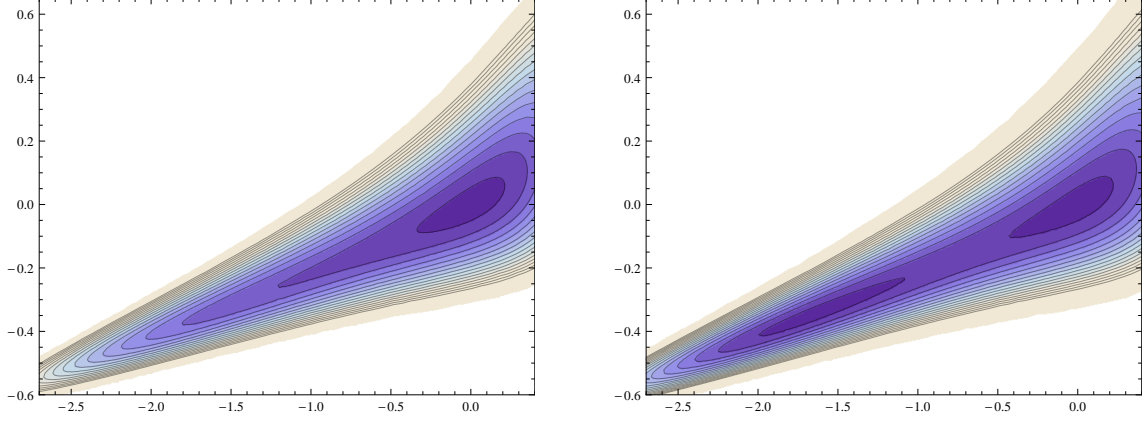


Figure 10: Contour plots of the bion- and monopole-instanton-induced potential V_{total} for G_2 for subcritical and critical values of c_m (the gaugino mass), as a function of b'_1 and b'_2 (at $\theta = 0$). Left panel: Contour plot of the potential for $c_m < c_m^{**} < c_m^{cr}$ ($c_m = 1.4$, $c_m^{cr} = 1.587$). The minimum at the origin ($\langle \vec{b}' \rangle = 0$, $\langle \vec{\sigma}' \rangle = 0$) is unique and not destabilized by monopole-instantons. The vacuum energy is $-5.6V_{bion}^0$. Right panel: Contour plot of the potential for $c_m = c_m^{cr} = 1.587$. The minimum at the origin is degenerate with the $\langle \vec{b}' \rangle = (-1.648, -0.345)$, $\langle \vec{\sigma}' \rangle = 0$ minimum. The vacuum energy is $-6.348V_{bion}^0$.

of the potential vanishes. It is also straightforward to see that this point is an extremum and that the masses of \vec{b}' and $\vec{\sigma}'$ excitations are identical, as required by supersymmetry. When the gaugino mass is turned on, $c_m \neq 0$, the three kinds of monopole-instantons associated with the affine and simple roots generate the terms in the potential given on the last three lines in Eq. (4.4). These terms can be obtained by a calculation, valid at $mL \ll 1$, virtually identical to that of Appendix B of [1], where the $SU(2)$ case was considered.

Let us now analyze the minima of the total potential in Eq. (4.4). In doing so, we shall ignore the $\mathcal{O}(g^2)$ terms in the monopole-instanton induced potential. This is consistent in the weak-coupling limit. These terms will contribute a shift of the vevs of \vec{b}' and $\vec{\sigma}'$ of order g^2 , which can further induce an order g^4 shift in $\langle \Omega \rangle$, which we ignore. As in the discussion of the $SU(N_c)$ case, we first study the expansion of Eq. (4.4) to quadratic order around $\langle \vec{b}' \rangle = \langle \vec{\sigma}' \rangle = 0$ and find that a sufficiently large c_m (a number of order unity) destabilizes the supersymmetric ground state. It is also easy to see that, as in $SU(N_c > 2)$, there are cubic terms in the potential for the \vec{b}' fields. Thus, one expects a discontinuous transition to a ground state where the field \vec{b}' acquires a vev (and perhaps also $\vec{\sigma}'$). To locate the transition we study the $\theta = 0$ case in more detail. In this case the $\langle \vec{b}' \rangle = \langle \vec{\sigma}' \rangle = 0$ vacuum with $k = 0$ has the lowest energy. We find that for $c_m < c_m^{cr} \approx 1.587$ the supersymmetric vacuum is stable. At $c_m = c_m^{cr}$, a metastable vacuum with $\langle b'_1 \rangle = -1.648$, $\langle b'_2 \rangle = -0.345$, $\langle \vec{\sigma}' \rangle = 0$ becomes degenerate with the zero-vev ground state. Contour plots of the potential are shown in Figure 10.

We find that while there is no symmetry associated with the discontinuous transition to a new vacuum at $c_m > c_m^{cr}$, the value of $\langle \text{tr} \Omega \rangle$ changes discontinuously from its subcritical

value (4.3):

$$\begin{aligned}
c_m < c_m^{cr} &: \langle \text{tr}\Omega \rangle = -0.15 \frac{g^2}{4\pi}, \\
c_m = c_m^{cr+} &: \langle \text{tr}\Omega \rangle = 3.21 \frac{g^2}{4\pi}.
\end{aligned}
\tag{4.7}$$

To obtain the second number above, we substituted the expectation value of $\langle \vec{\phi} \rangle$, Eq. (4.2) with the vevs of \vec{b}' as given in the previous paragraph, into Eq. (4.1). It is interesting to compare Eq. (4.7) to the results obtained in the lattice simulations of pure Yang Mills G_2 theory [36, 38]. Fig. 4 of Pepe et al. [36] shows histograms of $\langle \text{tr}\Omega \rangle$ in the low and high temperature phase. The results show that $\langle \text{tr}\Omega \rangle$ changes from slightly negative values below T_c to large positive values above T_c , in agreement with Eq. (4.7).

5. Weak vs. strong coupling non-trivial Wilson line holonomy

We would like to conclude with a general discussion of the relation between semi-classical theories of confinement, discussed in this work, and strong coupling confinement, studied on the lattice. For simplicity we consider $SU(N_c)$ gauge theory. A question that is not well understood is whether the expectation value of the trace of the Wilson line vanishes in the confined phase because

- a) the Wilson line is dominated by gauge configurations in which its eigenvalues are located at the N_c roots of unity with small fluctuations around them. This is the adjoint Higgs regime, see Fig. 3b.
- b) fluctuations randomize the eigenvalues over the unit circle, and there is no preferred background, as in Fig. 3c.

This question is a source of confusion especially when one considers the phase transition in pure YM theory. There, the transition occurs at the strong scale, hence there is no parametric separation of scales to justify an effective field theory in the transition regime.⁹ This regime is often *modelled* by a potential which breaks the center symmetry in the high temperature deconfined phase and restores it in the low temperature confined phase. In the limit of asymptotically high T the potential can be justified via a perturbative calculation [3], but at low T the coupling is strong and one cannot systematically derive a potential. Ref. [41] discusses this issue and proposes that option a) is operative in the low T confined regime of Yang-Mills theory; note that this point of view is also taken in [39] and [42].

First, we emphasize that *both a) and b)* take place in the confined phase of a large class of gauge theories on $\mathbb{R}^3 \times \mathbb{S}_L^1$, where \mathbb{S}_L^1 is a spatial circle. Examples include $\mathcal{N} = 1$ SYM and

⁹An exception is the second order transition of pure $SU(2)$ gauge theory. In this case universality arguments imply the existence of a $3d$ effective theory for the Wilson line [43]. We also note that one can always define an effective potential for the Wilson line. This potential simply determines the free energy as a function of the average Wilson line — it is not the potential in a local effective field theory.

QCD(adj), deformed-YM, and deformed-QCD. In all these theories, there are two types of confinement operative for different ranges of the parameters. We have

$$\begin{aligned} \frac{LN_c\Lambda}{2\pi} \ll 1, & \quad \text{abelian confinement, } a) \text{ is operative,} \\ \frac{LN_c\Lambda}{2\pi} \gg 1, & \quad \text{non-abelian confinement, } b) \text{ is operative.} \end{aligned} \quad (5.1)$$

The small parameter $\frac{LN_c\Lambda}{2\pi} \ll 1$ arises in the abelian confinement regime as the separation of scales between the heaviest dual photon mass m_σ which is degenerate with m_b given in Eq. (2.18) and lightest W -boson mass m_W :

$$\frac{m_\sigma}{m_W} \approx \left(\frac{\Lambda}{m_W}\right)^3 \log \frac{\Lambda}{m_W} \ll 1, \quad (5.2)$$

implying the first line of Eq. (5.1). This is the regime of abelian confinement where an adjoint Higgs mechanism is operative and weak coupling non-trivial holonomy shown in Fig. 3b is valid. In this regime, the fluctuations of the eigenvalues are much smaller than the typical eigenvalue separation. Once this hierarchy is lost there is no longer an adjoint Higgs effect: the eigenvalues have large fluctuations and are essentially randomized over the unit circle. We call this the regime of strong coupling non-trivial holonomy, see the discussion in Ref. [21].

There is some evidence from lattice simulations that the transition in pure Yang Mills theory is between a phase with weak coupling trivial holonomy as in Fig. 3a) and a strong coupling non-trivial holonomy shown in Fig. 3c). Fig. 2 of Ref. [44] shows the free energy of parameterized Wilson lines $\Omega = \text{Diag}(e^{i\pi\nu}, e^{-i\pi\nu})$ in pure gauge $SU(2)$ for different temperatures. At high temperature the free energy agrees with the perturbative one-loop potential and has a minimum at $\nu = 0$. On the other hand, the free energy in the low temperature does not have a pronounced minimum at $\nu = \frac{1}{2}$. Instead, the free energy is essentially ν independent, suggesting that the Wilson line averages to zero because of the large fluctuations of ν in the confined phase.

5.1 What changes between the semi-classical and strongly coupled deconfinement transitions?

The phase diagram shown in Fig. 1 contains both types of transitions. The transition from the deconfined phase to abelian confinement at small $L\Lambda$ continuously evolves to a transition to non-abelian confinement at $L\Lambda \sim 1$. Properties of the phase transition that can be studied reliably in the abelian regime can be extrapolated to the non-abelian regime. One may wonder whether one can improve upon this, and find a more direct connection between deconfinement transition in the abelian and non-abelian regime.

In the semi-classical limit neutral bions $\mathcal{B}_{ii} = [\mathcal{M}_i \overline{\mathcal{M}}_i]$ provide repulsion between the eigenvalues of the Wilson line. It is not hard to see that magnetic bion-anti-bion configurations, 4-defects, such as $[\mathcal{B}_{ij} \overline{\mathcal{B}}_{ij}] \equiv [\mathcal{B}_{ij} \mathcal{B}_{ji}]$ also generate repulsion among eigenvalues, and the same is true for 6-defects $[\mathcal{B}_{ij} \mathcal{B}_{jk} \mathcal{B}_{ki}]$. In the semi-classical regime these effects are exponentially suppressed relative to bions. Recent works provide evidence that these molecular configurations are semi-classical realizations of IR-renormalons [14, 45]. In particular,

in the complex Borel-plane, molecular events are associated with singularities located at $t_n^{sc.l.} \sim \frac{2S_L}{N_c} n$, $n = (1), 2, 3, \dots$, where the existence of the $n = 1$ term depends on details of the particular theory. Note that the location of the singularities is smaller by a factor $1/N_c$ relative to the instanton-anti-instanton singularity, and that they survive the large- N_c limit discussed in Section 2.1. The location of the infrared renormalon poles for the theory on \mathbb{R}^4 , or for the center-symmetric theory on $\mathbb{R}^3 \times \mathbb{S}_L^1$ in the $\frac{LN_c\Lambda}{2\pi} \gg 1$ domain, is given by $t_n \sim \frac{2S_L}{\beta_0} n$, $n = (1), 2, 3, \dots$, where again, the existence of the $n = 1$ term depends on the theory, and $\beta_0 = 3N_c$ for SYM and $\beta_0 = \frac{11}{3}N_c$ for YM. The crucial point is that both types of singularities appear with a factor of $\frac{1}{N_c}$ up to order one pre-factors. The order one pre-factors is what seems to be changing as one moves on from the abelian to non-abelian confinement regime, and by adiabatic continuity, the IR-renormalons in the strongly coupled phase transition replace the role of neutral bions in the semi-classical regime. We believe that this direction is worthy of further investigation.

6. Prospects

In this work, we provide a microscopic mechanism for the deconfinement phase transition in a weakly coupled setting which is continuously connected to the phase transition in pure gauge Yang Mills theory with any gauge group. We find that the mechanism for the phase transition is universal, independent of the symmetries of the gauge group. Neutral bions generate repulsion among eigenvalues of Wilson line, and this effect is counter-acted by the perturbative one-loop potential and monopole-instantons which generate an attraction. In the weak coupling regime the calculation is based on the semi-classical expansion, and the results can be checked (except in the case $\theta \neq 0$) using lattice simulations. It may be possible to extend some of the calculations beyond the semi-classical regime using resurgence theory and transseries, see [14].

The exact counterpart of our analysis can be carried out to describe the deconfinement phase transition or rapid crossover in two-dimensional non-linear sigma models, for example the $O(N)$ and $CP(N-1)$ models, or the chiral principal model. Starting with a supersymmetric version of these theories on $\mathbb{R} \times \mathbb{S}_L^1$, and turning on a mass term for the fermions, a semi-classical transition takes place. We claim that the neutral bions (correlated kink-antikink instanton events in that context) are the universal topological configurations leading to the confined regime of these theories.

There are several possible lines of investigation that can be pursued in the future. One is the goal to extend our calculations into the strongly coupled regime along the lines discussed in the previous section, by studying the singularity structure in the Borel plane both in the confined and deconfined phases. Another direction of study is more detailed investigations of confinement in the semi-classical regime, for example by constructing effective theories for abelian strings, or for the domain walls that separate the different k -vacua. In addition to that we are of course interested in experimental manifestations of the confinement mechanism. A recent set of ideas that promises to link deconfinement with the role of topological objects is the chiral magnetic effect [46]. This effect leads, in the deconfined phase, to electric charge separation in a large magnetic field, in the presence of topological configurations that can

generate net chirality. The effect is suppressed by the small density of 4d instantons in the high temperature phase, $\sim \exp[-8\pi^2/g^2]$. The density of monopole-instantons scales as $\exp[-8\pi^2/(g^2 N_c)]$, which may result in an enhancement of the chiral magnetic effect.

Acknowledgments

This work was supported in part by the US Department of Energy grants DE-FG02-03ER41260 (T.S.), DE-FG02-12ER41806 (M.Ü.), and the National Science and Engineering Research Council of Canada (E.P.). E.P. thanks the Tata Institute for Fundamental Research, Mumbai, for hospitality during the completion of this paper.

References

- [1] E. Poppitz, T. Schäfer and M. Ünsal, “Continuity, Deconfinement, and (Super) Yang-Mills Theory,” *JHEP* **1210**, 115 (2012) [arXiv:1205.0290 [hep-th]].
- [2] E. Poppitz and M. Ünsal, “Seiberg-Witten and Polyakov-like magnetic bion confinements are continuously connected,” *JHEP* **1107**, 082 (2011) [arXiv:1105.3969 [hep-th]].
- [3] D. J. Gross, R. D. Pisarski and L. G. Yaffe, “QCD and instantons at finite temperature,” *Rev. Mod. Phys.* **53**, 43 (1981).
- [4] N. Seiberg and E. Witten, “Gauge dynamics and compactification to three-dimensions,” Proceedings of the conference on mathematical beauty of physics, Saclay, France (1996), page 333-366 [hep-th/9607163].
- [5] O. Aharony, A. Hanany, K. A. Intriligator, N. Seiberg and M. J. Strassler, “Aspects of N=2 supersymmetric gauge theories in three-dimensions,” *Nucl. Phys. B* **499**, 67 (1997) [hep-th/9703110].
- [6] N. M. Davies, T. J. Hollowood and V. V. Khoze, “Monopoles, affine algebras and the gluino condensate,” *J. Math. Phys.* **44**, 3640 (2003) [hep-th/0006011].
- [7] M. Ünsal and L. G. Yaffe, “Large-N volume independence in conformal and confining gauge theories,” *JHEP* **1008**, 030 (2010) [arXiv:1006.2101 [hep-th]].
- [8] K. -M. Lee, P. Yi, “Monopoles and instantons on partially compactified D-branes,” *Phys. Rev. D* **56**, 3711-3717 (1997). [hep-th/9702107].
- [9] T. C. Kraan and P. van Baal, “Monopole constituents inside $SU(n)$ calorons,” *Phys. Lett. B* **435**, 389 (1998) [arXiv:hep-th/9806034].
- [10] T. M. W. Nye and M. A. Singer, “An \mathcal{L}^2 -index theorem for Dirac operators on $\mathbb{R}^3 \times \mathbb{S}^1$,” *J. Funct. Anal.* **177**, 203 (2000) [arXiv:math/0009144].
- [11] E. Poppitz and M. Ünsal, “Index theorem for topological excitations on $\mathbb{R}^3 \times \mathbb{S}^1$ and Chern-Simons theory,” *JHEP* **0903**, 027 (2009) [arXiv:0812.2085 [hep-th]].
- [12] M. Ünsal, “Magnetic bion condensation: A new mechanism of confinement and mass gap in four dimensions,” *Phys. Rev. D* **80** (2009) 065001 [arXiv:0709.3269 [hep-th]].
- [13] M. M. Anber, E. Poppitz, “Microscopic structure of magnetic bions,” *JHEP* **1106**, 136 (2011). [arXiv:1105.0940 [hep-th]].

- [14] P. C. Argyres, and M. Ünsal, “The semi-classical expansion and resurgence in gauge theories: new perturbative, instanton, bion, and renormalon effects,” JHEP **1208**, 063 (2012) [arXiv:1206.1890 [hep-th]].
- [15] B. Lucini, M. Teper and U. Wenger, “Properties of the deconfining phase transition in SU(N) gauge theories,” JHEP **0502**, 033 (2005) [hep-lat/0502003].
- [16] M. Panero, “Thermodynamics of the QCD plasma and the large-N limit,” Phys. Rev. Lett. **103**, 232001 (2009) [arXiv:0907.3719 [hep-lat]].
- [17] A. Mykkanen, M. Panero and K. Rummukainen, “Casimir scaling and renormalization of Polyakov loops in large-N gauge theories,” JHEP **1205**, 069 (2012) [arXiv:1202.2762 [hep-lat]].
- [18] B. Lucini and M. Panero, “SU(N) gauge theories at large N,” arXiv:1210.4997 [hep-th].
- [19] J. Beringer *et al.* [Particle Data Group Collaboration], “Review of Particle Physics (RPP),” Phys. Rev. D **86**, 010001 (2012).
- [20] E. Witten, “Theta dependence in the large N limit of four-dimensional gauge theories,” Phys. Rev. Lett. **81**, 2862 (1998) [hep-th/9807109].
- [21] M. Ünsal and L. G. Yaffe, “Center-stabilized Yang-Mills theory: Confinement and large N volume independence,” Phys. Rev. D **78**, 065035 (2008) [arXiv:0803.0344 [hep-th]].
- [22] B. Bringoltz and M. Teper, “In search of a Hagedorn transition in SU(N) lattice gauge theories at large-N,” Phys. Rev. D **73**, 014517 (2006) [hep-lat/0508021].
- [23] N. Cabibbo and G. Parisi, “Exponential Hadronic Spectrum and Quark Liberation,” Phys. Lett. B **59**, 67 (1975).
- [24] C. B. Thorn, “Infinite N_c QCD at finite temperature: Is there an ultimate temperature?,” Phys. Lett. B **99**, 458 (1981).
- [25] T. D. Cohen, “QCD strings and the thermodynamics of the metastable phase of QCD at large $N(c)$,” Phys. Lett. B **637**, 81 (2006) [hep-th/0602037].
- [26] O. Aharony, J. Marsano, S. Minwalla, K. Papadodimas and M. Van Raamsdonk, “The Hagedorn - deconfinement phase transition in weakly coupled large N gauge theories,” Adv. Theor. Math. Phys. **8**, 603 (2004) [hep-th/0310285].
- [27] O. Aharony, J. Marsano, S. Minwalla, K. Papadodimas and M. Van Raamsdonk, “A First order deconfinement transition in large N Yang-Mills theory on a small S^3 ,” Phys. Rev. D **71**, 125018 (2005) [hep-th/0502149].
- [28] J. C. Myers and M. C. Ogilvie, “New phases of SU(3) and SU(4) at finite temperature,” Phys. Rev. D **77**, 125030 (2008) [arXiv:0707.1869 [hep-lat]].
- [29] M. C. Ogilvie, “Phases of Gauge Theories,” J. Phys. A **45**, 483001 (2012) [arXiv:1211.2843 [hep-th]].
- [30] M. D’Elia and F. Negro, “ θ dependence of the deconfinement temperature in Yang-Mills theories,” Phys. Rev. Lett. **109**, 072001 (2012) [arXiv:1205.0538 [hep-lat]].
- [31] E. Vicari and H. Panagopoulos, “Theta dependence of SU(N) gauge theories in the presence of a topological term,” Phys. Rept. **470**, 93 (2009) [arXiv:0803.1593 [hep-th]].
- [32] E. Thomas and A. R. Zhitnitsky, “Topological Susceptibility and Contact Term in QCD. A Toy Model,” Phys. Rev. D **85**, 044039 (2012) [arXiv:1109.2608 [hep-th]].

- [33] M. Ünsal, “Theta dependence, sign problems and topological interference,” *Phys. Rev. D* **86**, 105012 (2012) [arXiv:1201.6426 [hep-th]].
- [34] M. M. Anber, “Theta dependence of the deconfining phase transition in pure $SU(N_c)$ Yang-Mills theories,” arXiv:1302.2641 [hep-th].
- [35] K. Holland, P. Minkowski, M. Pepe and U. J. Wiese, “Exceptional confinement in $G(2)$ gauge theory,” *Nucl. Phys. B* **668**, 207 (2003) [hep-lat/0302023].
- [36] M. Pepe and U. -J. Wiese, “Exceptional Deconfinement in $G(2)$ Gauge Theory,” *Nucl. Phys. B* **768**, 21 (2007) [hep-lat/0610076].
- [37] J. Greensite, K. Langfeld, S. Olejnik, H. Reinhardt and T. Tok, “Color Screening, Casimir Scaling, and Domain Structure in $G(2)$ and $SU(N)$ Gauge Theories,” *Phys. Rev. D* **75**, 034501 (2007) [hep-lat/0609050].
- [38] G. Cossu, M. D’Elia, A. Di Giacomo, B. Lucini and C. Pica, “ $G(2)$ gauge theory at finite temperature,” *JHEP* **0710**, 100 (2007) [arXiv:0709.0669 [hep-lat]].
- [39] D. Diakonov and V. Petrov, “Confinement and deconfinement for any gauge group from dyons viewpoint,” *AIP Conf. Proc.* **1343**, 69 (2011) [arXiv:1011.5636 [hep-th]].
- [40] E. -M. Ilgenfritz and A. Maas, “Topological aspects of $G2$ Yang-Mills theory,” arXiv:1210.5963 [hep-lat].
- [41] A. Dumitru, Y. Guo, Y. Hidaka, C. P. K. Altes and R. D. Pisarski, “Effective Matrix Model for Deconfinement in Pure Gauge Theories,” *Phys. Rev. D* **86**, 105017 (2012) [arXiv:1205.0137 [hep-ph]].
- [42] E. Shuryak and T. Sulejmanpasic, “The Chiral Symmetry Breaking/Restoration in Dyonic Vacuum,” *Phys. Rev. D* **86**, 036001 (2012) [arXiv:1201.5624 [hep-ph]].
- [43] B. Svetitsky and L. G. Yaffe, “Critical Behavior at Finite Temperature Confinement Transitions,” *Nucl. Phys. B* **210**, 423 (1982).
- [44] D. Diakonov, C. Gattringer and H. -P. Schadler, “Free energy for parameterized Polyakov loops in $SU(2)$ and $SU(3)$ lattice gauge theory,” *JHEP* **1208**, 128 (2012) [arXiv:1205.4768 [hep-lat]].
- [45] P. Argyres and M. Ünsal, “A semiclassical realization of infrared renormalons,” *Phys. Rev. Lett.* **109**, 121601 (2012) [arXiv:1204.1661 [hep-th]].
- [46] K. Fukushima, D. E. Kharzeev and H. J. Warringa, “The Chiral Magnetic Effect,” *Phys. Rev. D* **78**, 074033 (2008) [arXiv:0808.3382 [hep-ph]].